SCUOLA DI DOTTORATO
UNIVERSITÀ DEGLI STUDI DI MILANO-BICOCCA

Department of

SCHOOL OF MEDICINE AND SURGERY

PhD program in TRANSLATIONAL AND MOLECULAR MEDICINE Cycle XXXI

In vitro models for studying oxaliplatin neurotoxic effects

Surname MONZA Name LAURA
Registration number 710555

Tutor: BECCHETTI ANDREA

Co-tutor: LECCHI MARZIA

Coordinator: BIONDI ANDREA

ACADEMIC YEAR 2017/2018

TABLE OF CONTENTS

1. INTRODUCTION

1.1 Chemoteraphy-induced peripheral neurotoxicity

In the last few years, as a result of the advancements in early diagnosis and in the efficacy of oncological treatments, there has been an increase in the number of patients cured from cancer and in the amount of patients with long-term survival (Henley et al., 2017; Siegel et al., 2017). Consequently, the attention has been focused on the persistent side effects of cancer treatment that may affect the patient quality of life (Argyriou et al., 2012) and increase the annual cost of healthcare (Pike et al., 2012).

Among the others, the chemotherapy-induced peripheral neurotoxicity (CIPN) represents one of the most common and potentially dose-limiting adverse events associated with the use of anticancer drugs most commonly employed as adjuvant or primary treatment for breast, colorectal, head and neck, lung, ovarian, hematological and testicular cancer (Park et al., 2013). All these antineoplastic agents have a different chemical structure and mechanism of action and include: the platinum derivatives (like cisplatin and oxaliplatin), the vinka alkaloids (particularly vincristine and vinblastine), the taxanes (paclitaxel, docetaxel), the proteasome inhibitors (bortezomib and carfilzomib), the epothilones (ixabepilone) and immunomodulatory drugs (thalidomide) (Wolf et al., 2008; Brewer et al., 2016) (**Table 1**).

A recent meta-analysis conducted by Serenity et al. (2014) showed that the overall prevalence of CIPN is approximately 68% within the first month of treatment, around 60% at 3 months and 30% at 6

months or more. Moreover, the 40% of patients experience permanent symptoms (Park et al.; 2013). The prevalence of CIPN is specific for the anticancer drug used (Seretny et al., 2014).

Drug name	Type of cancer treated	Mechanism of action	Neuropathy incidence
Platinum-based drugs	Lung, ovarian, bladder, germ cells, testicular, colorectal cancer.	Cancer cell DNA-cross-linking.	70-100 %
Taxanes	Breast, ovarian, lung, prostate, pancreatic cancer.	Cancer cell microtubule formation impairment.	11-87 %
Thalidomide and its analogs	Multiple myeloma.	Antiangiogenesis, immunomodulation.	20-60 %
Ixabepilone	Breast cancer.	Tubulin malformation.	60-65 %
Bortezomib	Multiple myeloma.	Proteasome inhibition.	20-30 %
Vinca alkaloids	Lung, brain, bladder, testicular cancer.	Cancer cell microtubule formation.	Up to 20 %

Table 1. Characteristics of neurotoxicity-inducing drugs routinely used in clinical practice (Banach et al., 2016).

Generally, the clinical signs associated with CIPN are a peripheral neuropathy with a 'stocking and glove' distribution mainly characterized by sensory loss, paresthesia, dysesthaesia, numbness and tingling associated with neuropathic pain only in the most severe cases (Park et al., 2008; Jaggi and Singh, 2012). Motor symptoms, like weakness, autonomic neuropathy and cranial nerve involvement are less commonly reported (Miltenburg and Boogerd, 2014; Cavaletti, Alberti and Marmiroli, 2015).

The signs of CIPN are typically dose-dependent and can emerge after a single or cumulative doses at any time after the initiation of treatment, from hours to weeks or even months, and may continue post-therapy (Brewer et al., 2016).

The main clinical features of peripheral neurotoxicity associated with the chemotherapy drugs discussed above are summarized in **Table 2.**

Drug	Typical Symptoms/Signs
Platinum	
Cisplatin	Early reduction/loss deep tendon reflexes. Distal, symmetric, upper- and lower-limb impairment/loss of all sensory modalities. Sensory ataxia and gait imbalance are frequent. Neuropathic pain can be present, but is it not frequent. Coasting phenomenon is frequent.
Carboplatin	Similar to cisplatin but milder
Oxaliplatin	Acute: cold-induced transient paresthesias in mouth, throat and limb extremities; cramps/muscle spasm in throat muscle, jaw spasm. Chronic: very similar to cisplatin.
Bortezomib	Reduction/loss deep tendon reflexes. Mild to moderate, distal symmetric loss of all sensory modalities occurs. Small myelinated and unmyelinated fibers are markedly affected, leading to severe neuropathic pain. Mild distal weakness in lower limbs is possible.
Taxanes (paclitaxel, docetaxel)	Reduction/loss deep tendon reflexes. Myalgia syndrome is frequent (as an atypical neuropathic pain?). Distal, symmetric, upper- and lower-limb impairment/loss of all sensory modalities. Gait unsteadiness is possible because of proprioceptive loss. Distal, symmetric weakness in lower limbs is generally mild.
Epothilones (ixabepilone, sagopilone)	Signs and symptoms are similar to taxanes, but neuropathic pain is less frequent, and recovery is reportedly faster.
Vinca alkaloids (Vincristine, other compounds)	Reduction/loss deep tendon reflexes. Neuropathic pain/paresthesia at limb extremities is relatively frequent. Distal, symmetric, upper- and lower-limb impairment/loss of all sensory modalities. Distal, symmetric weakness in lower limbs progressing to foot drop. Autonomic, symptoms may be severe.
Thalidomide	Reduction/loss deep tendon reflexes. Relatively frequent neuropathic pain at limb extremities. Mild to moderate, distal, symmetric loss of all sensory modalities. Weakness is rare.

Table 2. Typical clinical features of CIPN associated with conventional chemotherapy (Cavaletti, Alberti and Marmiroli, 2015).

These symptoms may be disabling and influence the patient's daily activities and quality of life (Canta et al., 2015; Hausheer et al., 2006).

Furthermore, these undesirable side effects can lead to dose modification, prolongation of the infusion time or early discontinuation of treatment that can increase cancer-related morbidity and mortality (Cavaletti and Marmiroli, 2010; Hershman et al., 2014). All these symptoms generally arise at limb extremities showing a distal to proximal progression (Cavaletti, Alberti and Marmiroli, 2015) and are caused by a damage to axons (length-dependent axonopathy) or to the cell bodies of dorsal root ganglia (DRG) neurons (neuronopathy) (Carozzi et al., 2015). The major susceptibility to the action of noxious exogenous agents of peripheral nervous system (PNS), compared to central nervous system (CNS), depends on its peculiar structure (Argyriou et al., 2012). In fact, the lack of a blood nerve barrier and the complexity of the processes involved in peripheral nerve repair and regeneration make DRGs and their axons susceptible to the collateral effects of cancer treatments (Allodi et al., 2012). Moreover, DRGs are characterized by the presence of dense vascularisation and fenestrated capillaries that make them even more sensitive to circulating molecules (Jimenez-Andrale, 2008). Damage to small sensory fibers occurs rarely with select chemotherapies (i.e. bortezmib), while large sensory fibers are the most commonly affected (Park et al., 2013; Cata et al., 2007).

While the mechanisms of action of the above mentioned antineoplastic drugs on tumor cells are relatively well established, little is known about their toxic activity and more studies are needed in order to find putative targets for the development of preventive and therapeutic strategies. However, over the past decade, several neurotoxic mechanisms have been proposed for the different classes

of anticancer drugs, which include: oxidative stress, mitochondrial damage, impaired axonal transport, dysfunction in sodium, potassium and Transient Receptor Potential (TRP) channels, neuroinflammation and selective cellular influx through specific transporters (Cavaletti and Marmiroli, 2015; Starobova and Vetter, 2017; Canta, 2015).

The identification of clinical and genetic risk factors for CIPN and the understanding of how they may impact on the response to antineoplastic treatment and on the onset of side effects is essential to identify susceptible patients (Addington and Freimer, 2016). Many factors that may increase the risk of CIPN onset and its severity have been identified, such as the specific antineoplastic drug used, the duration of exposure, cumulative dose, pre-existing history of neuropathy, combined therapies and genetic polymorphisms (Kerckhove et al., 2017). Other associated risk factors are represented by age, sex (female), race (black), history of diabetes, obesity, physical inactivity and metastatic versus non metastatic cancer (Kim and Johnson, 2017; Bakogeorgos and Georgouilias, 2017). On the other hand, a history of autoimmune disease seems to have a protective effect (Hershman et al., 2016).

The assessment of CIPN is frequently troublesome. In fact, there is no universally accepted assessment method that is based on both objective (i.e. clinical examination and nerve conduction studies, NCS) and subjective evaluations (neurotoxicity grading scales) (Miltenburg and Boogerd, 2014).
Conventional NCS is useful to evaluate the onset of CIPN but it only gives information about the involvement of large myelinated fibers

and does not detect changes in small fibers (Themistocleous et al., 2014).

Quantitative sensory testing and the measurement of nerve fiber density through corneal confocal microscopy and nociceptive-evoked potentials are useful tools for the evaluation of damages to small and unmyelinated nerve fibers (Verberne et al., 2013; Hoeijmakers et al., 2012). Magnetic resonance neurography is emerging as a new promising diagnostic tool that allows to visualize axonal alteration and demyelination (Wessing et al., 2011). In recent years, many different scales have been proposed to evaluate the grade of CIPN, such as the National Cancer Institute Common Toxicity Criteria scale and the Eastern Cooperative Oncology Group scale. These scales are easy to use but they usually underestimate the severity of symptoms (Cavaletti et al., 2010) and, therefore, they have been replaced by scales combining both clinical assessments and neurophysiological parameters like the Total Neuropathy Score (Cornblath et al., 2010).

Moreover, different self-reported questionnaires (Patient Reported Outcome Measures, PROM) have been developed and are increasingly used in neuroprotection clinical trials because they seem to be more accurate and sensitive compared to the clinician-reported ones (Alberti et al., 2014; Hershman et al., 2011).

Lastly, a recent preclinical study in a well-established rat model of vincristine-induced peripheral neurotoxicity proposed the dosage of serum neurofilament light chain (NfL) level as putative biomarker for CIPN severity (Meregalli et al., 2018). In fact, they showed that the progressive increase in serum NfL levels correlates with the progressive axonopathy. This simple approach could be easily

translated to clinical practice where careful monitoring of CIPN may be problematic (Cavaletti et al., 2013). However, additional studies are needed.

In spite of remarkable efforts on both preclinical and clinical side, no substantial progresses have been made in CIPN prevention and treatment that still represent unmet clinical needs (Staff et al., 2017; Bakogeorgos and Georgouilias, 2017). Cavaletti and Marmiroli (2018) stated that this worrisome situation seems to reflect a combination of methodological issues (i.e. the absence of a universally accepted assessment methods, the lack of reliable predictors of CIPN onset and severity able to identify high-risk subjects and the incomplete knowledge of the mechanisms underlying drug-induced neurotoxicity) and a lack of efficacy of the tested compounds. In fact, even if many preventive and therapeutic strategies have been attempted, including pharmacologic agents such as anticonvulsants (for example carbamazepine and pregabalin), antidepressants, chemoprotectants, vitamins, minerals and other dietary supplements (Bakogeorgos and Georgouilias, 2017), all these studies gave negative, conflicting or inconclusive results. For this reason, there are no available preventive strategies and, to date, the antidepressant duloxetine represents the only recommended treatment in patients with taxane or oxaliplatin (OHP) -induced peripheral neurotoxicity (Albers et al., 2014; Hershman et al, 2014). Therefore, treatment schedule modification still remains the only possible option to limit CIPN severity and its long-term/permanent symptoms (Mustafa et al., 2017).

1.2 Pre-clinical models for studying CIPN

Most of the information about the mechanisms underlying CIPN is based on the results obtained in studies conducted on preclinical models. These include both *in vivo* and *in vitro* models and are very useful in order to have a better insight of the pathophysiology of CIPN and to study the effects of putative neuroprotectants leading to new preventive and therapeutic strategies.

Over the last 20 years, a lot of chronic and acute animal models have been developed for the most important and widely used antineoplastic agents (Hopkins et al., 2016). They are usually established in rodents, mice or rats, but the use of non-mammalian models have been reported, although less frequently (zebrafish, Drosophila) (Fukuda et al., 2017). Chemotherapy drugs are usually administered to rodents through intraperitoneal or intravenous injection. The assessment of CIPN features is done using behavioural, electrophysiological, and histopathological (i.e. morphometric and morphological changes in DRGs and nerves and intraepidermal nerve fiber density) analysis conducted at different time points during the chemotherapy regimen (Hopkins et al., 2016).

Sensory and motor conduction studies of caudal and digital nerves represent a useful tool to evaluate the typical electrophysiological abnormalities observed in patients undergoing antineoplastic regimen (i.e. reduced nerve conduction velocity and compound action potential amplitude). More recently, nerve excitability testing (NET) has been translated from clinical to preclinical practice in order to study axonal hyperexcitability (George and Bostock, 2007). This technique may be

very important in evaluating possible neuroprotective strategies for the acute OHP related toxicity. Behavioral tests such as dynamic test, plantar test and cold plate test are used to evaluate pain-like behaviors that may be associated with CIPN (i.e. mechanical allodynia, and thermal hypo-and hyperalgesia).

Some of the critical aspects of CIPN animal models that may limit the translation of preclinical study results into clinical practice are represented by the proper reproduction of the chemotherapy regimen, the selected way of administration and assessment methods (Marmiroli et al., 2017).

Even if the rodent models of CIPN best resemble its clinical features, they are time consuming, expensive and their results may be difficult to interpret (Marmiroli et al., 2012). Moreover there is no standardization in the evaluation of CIPN and related neuropathic pain and this makes it difficult to compare data obtained in different laboratories (Fukuda et al., 2017). Based on these factors, *in vitro* models may be used as complementary tools for the study of CIPN pathophysiology and for the preliminary screening of new neuroprotectant molecules, reducing the number of compounds tested *in vivo* (Snyder et al., 2018).

At the beginning, CIPN mechanisms were investigated *in vitro* using cultures of differentiated neurons derived from tumoral cell lines, such as SH-SY5Y human neuroblastoma and rat PC12 pheocromocytoma cells (Nakagawa-Yagi et al., 2001; Villa et al., 2005; Geldof et al., 1998; Verstappen et al., 2004). These differentiated cells possess several properties of neuronal cells (Biedler et al., 1978; Sharma et al.,

1999) but lack a true neuronal phenotype (Marmiroli et al., 2012). For this reason, the mechanisms of CIPN and the effects of putative neuroprotectants were then studied on DRG neuron primary cultures and on co-cultures of DRG neurons and Schwann cells derived from embryonic or adult rats and mice (Gill and Windebank, 1998; Malgrange et al., 1994; Pittman et al., 2013; Imai et al, 2017). Recently, due to the advances in stem cell technology, the attention has been focused on the development of new *in vitro* models based on human neurons differentiated from induced pluripotent stem cells (iPSCs). Wainger et al. (2015) recently showed that nociceptor neurons deriving from human fibroblasts can be used to study the mechanisms underlying painful CIPN. Moreover, Wheeler et al. (2015) have demonstrated that human neuron-like cells derived from commercially available iPSCs can be used as a preclinical model to study anticancer drug neurotoxicity.

1.3 Platinum compounds

Chemotherapy based on platinum analogues represents the main treatment for many solid tumors including lung, colorectal, stomach, head and neck, cervix, oesophagus, bladder, ovarian and testicular cancer (Dasari and Tchounwou, 2014). The use of cisplatin (CDDP), carboplatin and OHP is approved worldwide while other platinum compounds as nedaplatin, heptaplatin and lobaplatin are approved only in Japan, South Korea and China respectively (Johnstone et al., 2016).

Platinum-based anticancer drugs are composed of doubly charged platinum ions surrounded by four ligands. The amine ligands allow the formation of stronger interactions with the platinum ion while the chloride ligands or carboxylate compounds constitute the leaving groups (**Figure 1**; Goodsell, 2006).

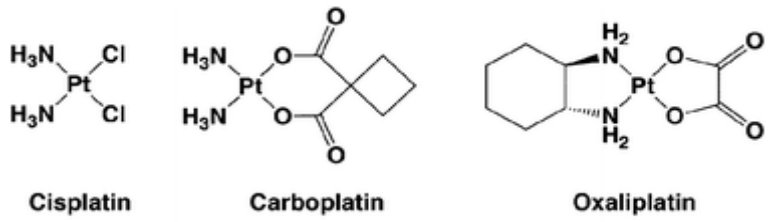

Figure 1. Chemical structure of the platinum-based anticancer drugs approved worldwide (Todd and Lippard, 2009).

All platinum compounds are administered intravenously in bolus or via slow infusion. They remain intact in the bloodstream and enter into cells through different mechanisms including passive diffusion through the plasma membrane and active transport mediated by membrane proteins such as copper transporters and/or organic cation

transporters (Johnstone et al., 2016; Lin et al., 2002; Howell et al., 2010, Puckett et al., 2010). Once in the cells, these drugs are aquated becoming highly reactive and thus forming adducts with the DNA and binding other cellular molecules such as proteins (Kelland, 2007). This mechanism is responsible not only for the anticancer activity of platinum analogues but also for their toxicity that depends on their poor selectivity for tumor cells. In fact, these compounds are up-taken also in other fast growing tissues leading to different, dose-dependent side effects that can be grouped in seven major categories: nephrotoxicity, ototoxicity, neurotoxicity, cardiotoxicity, hematological toxicity, hepatotoxicity and gastrointestinal toxicity (Oun et al., 2018). The incidence of all these adverse events varies depending on the platinum compound used. Although patients treated with platinum-based drugs experience similar side effects, the specific dose limiting toxicity is different for each compound of the class and is nephrotoxicity, myelosuppression and neurotoxicity for CDDP, carboplatin and OHP respectively (McWhinney et al., 2009).

The dosage used depends on different factors including: the cancer type, the protocol used, combined therapy and the patient's general status of health. Moreover, during chemotherapy regimen, the dose is adjusted taking into account the patient's body surface (Oun et al., 2018).

Cisplatin

CDDP (cis-diamminedichloroplatinum II) is the first developed platinum-based drug for chemotherapy. Its cytotoxic activity was accidentally discovered in 1965 by Rosenberg et al. while studying the

effects of alternating currents on the growth of *Escherichia Coli* (Rosenberg et al., 1965). Later on, its biological activity was tested in tumor bearing mice showing that it was able to induce marked tumor regression (Rosenberg et al. 1969). The first patient was treated with CDDP in 1971, and in 1978 the compound was approved for the treatment of testicular and ovarian tumors by the Food and Drug Administration (FDA) (Higby et al., 1974). To date, CDDP still represents a mainstay in the treatment of testicular, ovarian, bladder, cervical, head and neck and lung cancer (Weiss and Christian, 1993).

CDDP is composed of a central platinum ion surrounded by four ligands: two amines ligands and two chlorides as leaving groups (Goodsell, 2006). CDDP is administered intravenously and, once in the bloodstream, it is uptaken into the cytoplasm of cells by passive diffusion or via active transport. Upon entering a cell, the low concentration of chloride ions induces the loss of one or both leaving groups, that are replaced by water molecules through a series of spontaneous aquation reactions. The hydrolysis of CDDP results in the formation of a cationic platinum complex that is a very reactive molecule able to interact with nucleophilic sites (el-Khateeb et al., 1999; Kelland, 2000). In particular, CDDP interacts with nitrogens at nucleophilic N7-site of purine bases in DNA to form DNA-protein and DNA-DNA interstrand and intrastrand crosslinks (Eastman, 1987, Jamieson and Lippard, 1999). Intrastrand adducts are the major responsible for the cytotoxic action (Pinto and Lippard, 1985). In fact, 1,2-intrastrand ApG and GpG crosslinks account for 85-90% of total lesions (Kelland, 1993) while, the 1.3-interstrand (GpG) crosslinks and monofunctional adducts make up about 2-6% of the platinum

bound to DNA each (Siddik, 2003). These chemical alterations induce the distortion of the DNA double helix, introducing abnormal curvatures and unwindings that inhibit its replication and transcription (Imran et al., 2013). If the amount of damaged DNA exceeds the repair capability, the cell dies through apoptosis.

Despite its proven effectiveness as an antineoplastic drug, CDDP clinical use may be limited by tumor cell resistance and nephrotoxicity (Cerri et al., 2011). For these two reasons, second and third generation platinum compounds have been developed.

Carboplatin

Cis diammine (1,1-cyclobutanecarboxylato) platinum (II), carboplatin, is a second generation platinum compound developed to reduce the CDDP related side effects (Harrap, 1985). Differently from CDDP, carboplatin has a bidentate dicarboxylate ligand as a leaving group. This ligand is less labile compared to chloride ligands, reducing the aquation rate and thus the related toxicity. In fact, carboplatin has a safer profile compared to CDDP but also its antineoplastic efficacy is reduced (Knox et al., 1986). It is classified as an alkylating agent and it exerts its anticancer activity forming predominantly intrastrand DNA cross-links.

Carboplatin is used in combination with other chemotherapy drugs as part of first-line treatment for ovarian and lung cancer (Avan et al., 2015). Hematotoxicity, in particular myelosuppression, represents its dose limiting adverse reaction (Canetta et al., 1985).

Oxaliplatin

OHP, (1R,2R)-cyclohexane-1,2-diamine oxalate-platinum(II), is a third generation platinum-based compound developed to overcome cisplatin resistance (Mathé et al., 1989). It was firstly used in France in 1996, in 1999 it was introduced in whole Europe, and in 2002 in USA (Monneret, 2011). OHP is indicated, in combination with folinic acid (Leucovorin) and 5-fluorouracil (FOLFOX regimen), for first-line and adjuvant metastatic colorectal cancer therapy (Chau and Cunningham, 2003). In addition, it can be used in combination with capecitabine (XELOX/CAPOX regimen) and it has demonstrated its efficacy also against pancreatic and gastroesophageal cancers (Cassidy et al., 2004; Louvet et al., 2005; Cunningham et al., 2008). Differently from CDDP, it is composed of a central doubly charged platinum ion surrounded by a 1,2-diaminocyclohexane ligand (DACH) and an oxalate as a living group (Kelland, 2007). The bulky DACH ligand is responsible for the higher cytotoxicity of OHP compared to CDDP (Carozzi et al, 2015). In fact, although DACH confers on OHP a reduced cross-reactivity with DNA, its dimension prevents binding of the DNA mismatch repair proteins, which is a mechanism involved in resistance to alkilating-agents (Raymond et al., 1998). The oxalate leaving group reduces the severity of adverse events (Cassidy and Misset, 2002).

In the bloodstream, the oxalate group is rapidly displaced by chloride ions forming dichloro(DACH)platinum complexes that can enter the cells. Once inside the cells, where the chloride concentration is lower (4- 20 mM), these complexes are aquated ad thus converted to the active forms with cytotoxic activity (Alcindor and Beauger, 2011). In

GC-rich sites, they mainly form DNA intrastrand crosslink with a nitrogen atom of guanine, forming mono- and then diadducts (Faivre et al., 2003). These adducts inhibit DNA replication and transcription and thus lead to cell death through apoptosis (Di Francesco et al., 2002). Additionally, OHP can cause interstrand crosslinks and DNA-protein crosslinks (Zwellinget al., 1979).

Despite the absence of nephrotoxicity and drug resistance compared to CDDP and its proven antitumor activity, the clinical use of OHP may be limited by the onset of peripheral neurotoxicity.

1.3.1 Oxaliplatin-induced pheripheral neurotoxicity (OIPN)

Differently from the other platinum analogues, the OHP-induced peripheral neurotoxicity has unique characteristics. In fact, it is associated with two forms of neurotoxicity with different timing and symptoms profile: an acute, transient syndrome and a dose-limiting chronic sensory neuropathy (Grothey, 2003). The acute toxicity is a key feature of OHP neurotoxicity. It occurs in nearly all patients (85-95%) during or shortly after the infusion and generally resolves within a week (de Gramont et al., 2000; Hausheer et al., 2006). Patients complain paresthesias and dysesthesias located at limb extremities and at perioral region. Although less common, motor signs may occur including cramps, fasciculations and muscular spasm-like contractions (Wilson et al., 2002). These symptoms are induced or aggravated by cold exposure and increase in severity and duration with cumulative dosage (Grothey, 2003; de Gramont et al., 2000; Wilson et al., 2002). Infusion prolongation, and thus lower peak plasma concentration of OHP, can reduce their severity and incidence (Extra et al., 1998). In addition, it has been demonstrated that the acute OHP related toxicity is predictive for the development of chronic and cumulative sensory neuropathy (Argyriou et al., 2013; Valesco et al., 2014). In fact, these symptoms and related electrophysiological abnormalities are detected in about 78% of patients who subsequently develop the chronic OIPN (Krishnan et al., 2005). Based on this link, possible preventive or therapeutic strategies for the acute symptoms may reduce the severity and toxicity of the chronic ones.

In patients with acute toxicity, sensory nerve conduction studies reveal no effects on the amplitude of compound action potential and nerve

conduction velocity. Moreover, no signs of neurotoxicity has been found in sural nerve biopsies. On the other hand, the acute symptoms seem to be related to increased nerve excitability. In fact, needle electromyography examinations and motor nerve conduction studies reveal spontaneous high frequency discharges of motor fibres and repetitive compound motor action potentials in response to a single electrical stimulus in the following 24-48h after OHP infusion (Wilson et al., 2002; Lehky et al., 2004). These findings are further supported by the results on nerve excitability testing in patients after OHP infusion that demonstrate an increase of refractoriness in motor axons and a decrease of the same parameter in sensory axons (Krishnan et al., 2005, 2006; Park et al., 2009). Taken together, these findings provide evidence of alterations in voltage-dependent sodium channels although a possible role of voltage-dependent potassium channels is still on debate. Therefore, the mechanisms underlying acute OIPN still have to be fully elucidated.

Chronic OIPN develops progressively in about 70% of patients with cumulative doses exceeding 540 mg/m^2 (Cerosimo, 2005; Argyriou et al., 2013b). It is a sensory neuropathy with a "stocking and glove" distribution, characterized by non cold-induced dysesthesia and paresthesias of the extremities and dysfunction of fine sensory-motor coordination, that develops gradually and increases in intensity with cumulative doses (Hartmann and Lipp, 2003; Cavaletti and Zanna, 2002). These symptoms may progress to sensory ataxia and functional impairment severely affecting the patient's quality of life (Gamelin et al., 2002). Sensory nerve conduction studies show a reduction in sensory AP amplitude while sensory conduction velocities are

normally not affected in the majority of patients. In addition, there is no involvement of motor nerves (Miltenburg and Boogerd, 2014; Argyriou et al., 2014).

It has been estimated that the described symptoms related to chronic OIPN partially reverse in 80% of patients and resolve completely in about 40% of patients in 6-8 months after the last administration (Argyriou et al., 2008). However, two studies evaluating long term course of OHP neurotoxicity reported persistence of symptoms and signs up to 5-6 years in almost 35% of patients (Pietrangeli et al., 2006; Brouwers et al., 2009). Moreover, the so called "coasting phenomenon" (i.e. the worsening of symptoms) may occur after discontinuation of OHP treatment (Lehky et al., 2004).

Chronic OIPN seems to be related to the accumulation of OHP in DRGs leading to atrophy or loss of DRG sensory neurons and secondary axonopathy (Luo et al., 1999; Screnci et al., 2000). However more efforts are needed to better understand the mechanisms involved in its pathogenesis.

Dose reduction or discontinuation of chemotherapy treatment still remain the only available strategies. In fact, a Cochrane review recently analyzed 29 studies describing nine possible chemoprotective agents (i.e. acetylcysteine, amifostine, calcium and magnesium, diethyldithiocarbamate, glutathione, Org 2766, oxcarbazepine, retinoic acid or vitamin E) against platinum induced neuropathy. They concluded that, to date, none of the tested neuroprotectants is worth to be recommended for the prevention or mitigation of platinum compound side effects on the peripheral nervous system (Albers et al.,

2014). This opinion was also sustained by a group of experts who carried out a systematic literature research with the purpose to write a clinical practice guideline for the prevention and management of CIPN in survivors of adult cancer. They concluded that there is no consistent evidence to support the use of antiepileptic drugs, antidepressants, vitamins and antioxidants as preventive/therapeutic strategies against CIPN in clinical routine. Only duloxetine, an antidepressant, is slightly recommended in cancer patients experiencing CIPN (Hershman et al., 2014). However, unexpectedly, a putative therapeutic option able to eliminate neuropathic and depressive-like effects of OHP has been recently identified in rilouzole, a benzothiazole derivative, activator of TREK 1 and TRAAK channels used for the treatment for amyotrophic lateral sclerosis (Poupon et al., 2018).

Given the lack of preventive and therapeutic strategies, the identification of risk factors for the development of chronic OIPN represent a crucial clinical need. For this aim, a lot of risk and prognostic factors has been reported and related with the onset and severity of OIPN and include patients clinical characteristics (acute OIPN symptoms and comorbidities), neurophysiological and laboratory findings and pharmacogenetics factors (Pulvers and Marx, 2016).

1.3.2 Role of transporters in OIPN

The key mechanism responsible for OIPN is represented by OHP accumulation in DRG neurons. For this reason, deepening the knowledge in OHP membrane transporters could be important not

only for OHP therapeutic effects but also for understanding its toxicity. In fact, these transporters are expressed in peculiar organs and cellular types (renal proximal tubular epithelial cells, cells of the auditory apparatus and nerve cells) where they mediate platinum drug influx and accumulation, leading to toxicity. In particular it has been reported that the copper transporters, CTR1, Mate 1, Atap7a and b control CDDP, OHP and carboplatin accumulation in cells (Komatsu et al., 2000; Samimi et al., 2004; Liu et al., 2009; Fujita et al., 2018). Moreover, other *in vitro* studies has highlighted a role of Oct2 in CDDP and OHP transport (Zhang et al. 2006; Filipski et al., 2009; Burger et al., 2010; Sprowl et al.; 2013). Recently, it has been reported that the knockdown of Oct1 but not of Oct2 ameliorated peripheral neuropathy in OHP treated mice (Fujita et al., 2018). This last finding is also supported by another work testing the effects of ergothioneine (a substrate/inhibitor of Oct1) and L-carnitine (a substrate/inhibitor of Oct2). In fact, they reported that the co-administration with ergothioneine but not L-carnitine decreased the accumulation of OHP and the development of mechanical allodynia in OHP treated rats (Nishida et al., 2018).

1.3.3 Involvement of ion channels in the onset of acute OIPN

Bacause of the resemblances between the symptoms experienced by OHP treated patients and the clinical features produced by disorders of voltage-dependent channels, acute OIPN is described in literature as a channelopathy-like syndrome (Gamelin et al., 2002). In particular, it appears to act by dysregulating the nodal voltage-dependent sodium channels (Chiorazzi et al., 2015).

Voltage-dependent (Na_v) sodium channels are transmembrane ion channel proteins important for action potential generation and propagation in excitable cells. In fact, dysfunctions of these channels are related to different disorders such as epilepsy and neuropathic pain. The voltage-dependent sodium channel gene family comprises nine homologous members SCN1A to SCN11A, encoding for selective ion channels $Na_v1.1$ to $Na_v1.9$ (Eijkelkamp et al., 2012). These channels are differentially expressed and, based on sequence and function, they can be mainly divided in two groups: tetrodotoxin (TTX) sensitive and TTX-resistant (Rogers et al., 2006). The classification of voltage-dependent sodium channels is summarized in **Table 3**.

Name	Gene	TTX-sensitive	Localization
$Na_v1.1$	*SCN1A*	Yes	CNS, DRG
$Na_v1.2$	*SCN2A2*	Yes	CNS
$Na_v1.3$	*SCN3A*	Yes	Embryonic CNS, injured DRG
$Na_v1.4$	*SCN4A*	Yes	Skeletal muscle
$Na_v1.5$	*SCN5A*	Moderate	Heart, embryonic CNS
$Na_v1.6$	*SCN8A*	Yes	DRG, motor neurons
$Na_v1.7$	*SCN9A*	Yes	DRG, low levels in CNS
$Na_v1.8$	*SCN10A*	No	DRG
$Na_v1.9$	*SCN11A*	No	DRG, low levels in hippocampus

Table 3. Classification of voltage-dependent sodium channels (Rogers et al., 2006).

The effects of OHP on compound action potentials (CAP) was first studied by Adelsberger et al. in the early 2000 but its pathogenesis still needs to be elucidated. In this work they studied the effects of OHP, at concentrations ranging from 25 to 250 µM, on different rat

preparations (i.e. rat sural, peroneal and vagal nerve preparations, DRG and hippocampal neuron primary cultures). They showed that OHP application, for up to 90 minutes, increased the amplitude and duration of compound APs in myelinated fibers, caused repetitive firing in response to an electrotonic stimulus and it also broadened the nerve refractory. All these effects were absent in the presence of TTX 1µM and were completely reverted by the application of carbamazepine, suggesting that OHP neurotoxicity is linked to alterations of the activity of voltage-dependent sodium channels rather than voltage-dependent potassium channels. Moreover, they demonstrated that incubation of rat DRG neurons with OHP for 5 minutes induced an increase in sodium currents and a shift of the channel voltage-dependence towards more negative potentials. These effects were not observed in rat hyppocampal primary cultures, indicating that OHP acts on specific sodium channel isoforms (Adelsberger et al., 2000).

One year later, Grolleau et al. (2001) tested the effects of OHP (40-500 µM) and its two major metabolites, applied for 20 minutes intracellularly (i.e. through the pipette solution) or extracellularly (i.e. through the bath solution), on cockroach derived dorsal unpaired median neurons. They observed a reduction in spike amplitude due to a reduction of the voltage-dependent sodium channel current density and they concluded that this effect was caused by oxalate molecules resulting from OHP biotransformation. These latter are chelators of Ca^{+} and Mg^{2+} ions and thus they can alter the functional properties of voltage-dependent sodium channels inducing a prolonged open state of these channels leading to hyperexcitability.

An effect on voltage-dependent sodium channels was also described by Webster et al. (2005). In fact, they showed that the application of OHP 500 µM for up to 80 minutes increased evoked and spontaneous neurotransmitter release in motor nerve terminals of mouse phrenic nerve hemidiaphragm preparations. These effects were prevented by the application of TTX while the application of potassium channel blockers did not replicate the OHP effects on mouse phrenic nerve hemidiaphragm preparations. However, Benoit and colleagues (2006), working on frog myelinated axons treated with OHP in the range of 1-100 µM for 5-10 minutes, reported a dose-dependent decrease in both sodium and potassium voltage-dependent currents without any change in the current kinetics. In addition, the compound was able to shifted the voltage-dependent activation of both sodium and potassium channels towards more negative membrane potentials. A negative shift in the steady-state inactivation curve of the peak Na^+ current was also observed in the presence of OHP. In the authors' opinion these effects may lead to an increase of membrane excitability due to the generation of APs at more negative membrane potentials and a decrease in their duration.

A dose-dependent reduction of peak amplitude of voltage-dependent sodium currents was also reported by Wu et al. (2009), who studied the effects of OHP (30-100 µM for 2 minutes) on differentiated NG108-15 cells (mouse neuroblastoma x rat glioma). Moreover, they reported a slowing down of sodium current inactivation kinetics, a strong decrease of delayed-rectifier potassium currents and a reduction in AP amplitude. No effect was described on peak amplitude of L-type calcium currents. In a final set of experiments in HEK293T cells

expressing SCN5A, they observed a decrease in the peak amplitude of voltage-dependent sodium current and a slowing of sodium current inactivation kinetics, a further indication that OHP may have different effects on sodium channel isoforms.

In addition, some studies suggest a specific involvement of the $Na_v1.6$ isoform in the onset of acute OIPN. In fact Sittl and colleagues (2012) observed that this channel subtype is responsible for the enhanced resurgent and persistent sodium current in cooled large diameter DRG neurons treated with OHP (30 µM) for 90 minutes and for the induced burst of APs in cooled myelinated axons incubated with OHP (100 µM for 90 minutes). The incubation with OHP did not produced any effect on DRG neurons and peripheral nerves from $Scn8a^{med/med}$ mice, which lacked functional $Na_v1.6$. This conclusion is further supported by a preclinical study conducted in a mouse model of OHP-induced cold allodynia based on a single intraplantar injection of this antineoplastic agent (Deuis et al., 2013). Lastly, Lolignier et al. (2015) recently evidenced the importance of the $Na_v1.9$ isoform in the perception of cold allodynia caused by OHP administration.

The hypothesis of a major involvement of sodium channels is further supported by the abnormalities observed in patients during nerve conduction studies, electromyography recordings, studies of nerve hyperexcitability and the results of recent pharmacogenomics studies that led to the identification of polymorphisms in genes that encode for voltage-dependent sodium channels related to the onset of OIPN (Argyriou et al., 2017). In particular, it has been reported that SCN4A rs2302237 is predictive of the severity of acute OIPN and for the

development of the chronic one whereas another work highlighted that SCN9A rs6746030 is protective against grade 3 OIPN (Argyriou et al., 2013b; Sereno et al., 2017)

However, there is growing evidence supporting an involvement of voltage-dependent potassium channels in the pathogenesis of acute OIPN. A possible key role of potassium channels was first reported by Kagiava et al. (2008; 2013). Through whole-nerve or intra-axonal recordings of *ex-vivo* rat sciatic nerves treated with OHP (100 or 500 µM for up to 5 hours) they did not observe any effect on the amplitude and depolarization phase of evoked compound APs concluding that voltage-dependent sodium channels were not affected. In contrast they reported a dramatic and dose-dependent increase of the duration of the repolarization phase and of the repetitive firing following a single stimulus, and a more pronounced afterhyperpolarisation that are suggestive of an inhibitory effect on voltage-dependent potassium channels. Some of these findings were obtained even with lower concentrations of OHP (5 and 25 µM applied in the bath for up to 20 and 13 hours respectively), similar to the peak concentration values reached in the plasma of treated patients after a single infusion, even if with a significant delay.

These data are further supported by Sittl et al. (2010) who reported that a flupirtine-mediated enhancement of axonal potassium conductance was able to reduce the rat sural nerve hyperexcitability (i.e. flupirtine induced an increase in threshold current necessary to evoke a compound AP of 40% maximal amplitude, a decrease in magnitude and duration of compound APs after activity in response to

electrical stimulation caused by a 60 minute long exposure to OHP 10-30 μM). Kagiava et al. (2015) observed that the effects of OHP incubation (25 μM for up to 20h) on mouse sciatic nerve could be reverted by octanol, a gap junction inhibitor. This finding suggests that OHP administration may cause prolonged opening of gap junction channels and hemichannels thus leading to potassium accumulation in the periaxonal space and thus its osmotic swelling. The overall process described above leads to potassium channel dysfunction.

Moreover, it has been recently reported that OHP administration (2 mg/Kg for five consecutive days) induces a down regulation of Kv4.3 channel expression in rat trigeminal neurons. This effect was associated with a reduction of A-type current component of voltage-dependent potassium outward currents accompanied by an increase in membrane excitability (Viatchenko-Karpinski et al., 2018).

In contrast to these findings supporting a role of voltage-dependent potassium channels in the onset of acute OIPN, Broomand et al. (2009) reported no effects of OHP (60-1000 μM, for different exposure time ranging from 5 minutes to 12 h) and its monocholoro complex on voltage-dependent Shaker potassium channels expressed in *Xenopus oocytes*. The authors concluded that acute OIPN cannot be explained with general effects on channel voltage-dependence through direct interaction of OHP with the amino acid residues on ion channels surface. They propose that OIPN is most likely caused by a slowing inactivation of specific sodium channels.

Lastly, it has been recently reported that acute or 24h long OHP treatment (10-100μM) differentially modulates voltage-dependent

calcium channels and APs in rat small DRG neurons (Schmitt et al., 2018). In fact they showed that, differently from the acute incubation, the 24h long treatment significantly increased the expression and the current densities of L- and T-type voltage-dependent calcium channels. Moreover, an increase of AP amplitude and characteristics were described.

In conclusion, since the most accredited hypothesis underlying acute OIPN is hyperexcitability of sensory neurons, a great number of studies have investigated the effects of this platinum-based compound on voltage-dependent sodium and potassium channels, the main effectors of electrical neuronal activity. These works used different preparations and cellular models and administered OHP concentrations sometimes very different from the peak values observed in the blood of treated patients (i.e. 1.44 µg/ml, corresponding to 3.6 µM, after 2h infusion for a dose of 85 mg/m^2 and 2.59-3.22 µg/ml, corresponding to 6.8 – 8.11 µM, after 2h infusion for a dose of 130 mg/m^2, Ehrsson et al., 2002; Graham et al., 2000). Overall, different effects have been reported involving sodium, potassium and calcium channels sometimes with discordant outcomes. These effects are summarized in **table 4.**

***In vitro* model used**	**[OHP] and timing**	**Effects on ion channels**	**Effects on cellular/nerves electrical activity**	**Reference**
Sural, vagal and peroneal nerves	25-250 µM up to 90 min *Most of experiments done with OHP 250 µM	-	↑ amplitude and duration of CAPs. Repetitive firing. Legthened of the refractory period.	Adelsberger et al., 2000.
DRG neurons		↑ in INa^+. Block of the maximal amplitude.	-	

		Shift of the channel voltage-dependence towards more negative potentials. Slow down of the inactivation kinetics.		
Hippocampal neurons		No effects.		
Cockroach dorsal unpaired median neurons	40-500 µM for 20 min *Most of experiments done with OHP 500 µM	Dose-dependent ↓ of voltage-dependent INa^+ amplitude. No effects on high voltage activated ICa^{2+}.	↓ AP amplitude. With longer OHP incubation, ↓ amplitude of both depolarizing phase and posthyperpolarisation associated with an ↑ of AP duration.	Grolleau et al., 2001.
mouse phrenic nerve hemidiaphragm	500 µM up to 80 min	Multiple nerve-evoked endplate potentials and ↑ in spontaneous miniature endplate potential frequency. Inhibitors of small conductance Ca^{2+} - activated K^+ channels and delayed rectifier voltage-dependent K^+ channels fail to reproduce OHP-like effects excluding their role at the neuromuscular junction.		Webster et al., 2005.
Frog myelinated axons	1-100 µM for 5-10 min *Most of experiments done with OHP 10 and 100 µM	Dose-dependent ↓↓↓ of INa^+ and negative shifts in the voltage-dependence of activation and inactivation. No changes in the current kinetics. Less marked ↓ in IK^+ and dose-dependent shift of activation towards more negative potentials. No effects on current kinetics.		Benoit et al., 2006.
Differentiated NG108-15 neuronal cells	30 and 100 µM for 2 min	↓ in the peak amplitude of INa^+ and dose-dependent slowing of INa^+ inactivation. No effects on persistent INa^+. No effects on peak amplitude of L-type ICa^{2+}. ↓ in IK^+ amplitude. No changes in the current	↓ amplitude of CAP. No effects on CAP duration and membrane resting potential.	Wu et al., 2009.

		kinetics.		
HEK293T cells expressing SCN5A		↓ peak INa^+ amplitude. Slow-down of INa^+ inactivation	-	
Sural nerve preparation from WT and $Scn8a^{med/med}$ and heterozygous mice	100 µM For 90 min	-	Burst of CAPs in myelinated fibres in WT mice. ↓ current amplitude required to evoke a 40% CAP response during log-lasting depolarizing current pulse.	Sittl et al., 2012.
Cooled large diameter DRG neurons from WT and $Scn8a^{med/med}$ mice	30 µM for 90 min	↑ TTX-sensitive resurgent and persistent INa^+ amplitude. No effects on activation and fast inactivation time constant.	-	
Neuron derived ND7/23 cells transfected with murine $Na_v1.6r$ and β4	30 µM for >30 min	Voltage-dependent slowing of fast inactivation time constant at negative membrane potentials.	-	
Adult rat sciatic nerve	100 or 500 µM for up to 300 min 1-25 µM for up to 780-1200 min	-	No effects in the amplitude and rise-time of CAP. No effects on the depolarization phase. Dose-dependent ↑ in the repolarization phase of CAP, burst like response and strong afterhyperpolarization.	Kagiava et al., 2008.
Adult rat sciatic nerve	100 or 150 µM 1-5 h	-	No effects on the depolarization phase of CAP. No effects on the CAP amplitude. Broadening of the repolarization phase. Thus ↑ CAP duration. Dose and time-dependent effects on fiber firing response to short stimuli (three different firing	Kagiava et al., 2013.

			patterns identified)	
Adult rat sural nerve.	10-30 µM for 60 min	-	↑ duration of CAPs and prolonged duration and increased magnitude of CAP after-activity (effects aggravated by cooling). The application of flupirtine (10 µM) ↓ the magnitude and duration of later component of CAP after-activity.	Sittl et al., 2010.
Mouse *ex vivo* sciatic nerve.	25 µM	-	Time-dependent ↑ duration of evoked CAPs due to an ↑ in the repolarizing time. No effects on the duration of the depolarizing phase. No effects on CAP amplitude. Effects reverted by octanol in a dose-dependent way.	Kagiava et al., 2015.
Rat dissociated V2 trigeminal neurons	Rats treated with OHP ip on 5 consecutive days	↓ Kv4.3 channel expression in rat trigeminal neurons. ↓ of A-type K^+ current amplitude.	↑ in membrane excitability	Viatchenko-Karpinski et al., 2018.
*Xenopus*oocytes	60-1000 µM for 5min up to 12h	No effects on: I amplitude and I time course voltage-dependence of Shaker K channel.	-	Broomand et al., 2009.
Rat small DRG neurons	1-500 µM Acute	Dose-dependent ↓ of voltage-dependent ICa: ↓ L-type ICa ↓ P-/Q-type ICa ↓ T-type ICa No effects on N-type ICa. No effects on voltage-dependence Ca^{2+} channels subtypes.	-	Schmitt et al., 2018.
	10 or 100	↑ of voltage-	↑ AP amplitude	

	µM for 24h	dependent ICa density: No effect on N- and P-/Q-type ICa density ↑ T- and L-type ICa density. ↑ T- and L-type voltage-dependent Ca^{2+} channel protein levels.	↓ time-to-peak ↓ rise time ↓ duration time delay No effects on AP baseline and AP duration after 90% decay starting from the maximal peak.	

Table 4. Effects of OHP on voltage-dependent ion channels and PA characteristics referred by literature.

With regard to the effects of CDDP on voltage-dependent ion channels, it seems that calcium channels could play a key-role in CDDP toxicity.

Tomaszewky and Büsselberg (2006) showed that CDDP treatment, in the range of 1 to 100 µM, reduced peak and sustained voltage-dependent calcium currents in rat DRG neurons while no effects were reported on voltage-dependent sodium and potassium channels. Moreover, Leo et colleagues (2017) reported a subtype-specific effects of CDDP (0.01-50 µM) on N-type voltage-dependent calcium channels. Lastly, results from an *in vivo* study testing nerve excitability revealed a possible involvement of K_v.7 voltage-dependent potassium channels (Nodera et al., 2011).

1.4 Scope of the thesis

The results reported in literature regarding OIPN still do not elucidate the molecular mechanisms underlying its onset. Moreover, those studies were often conducted using high concentrations of OHP and produced partial and sometimes controversial characterizations.
For these reasons, our aim was to further investigate the acute effects of a more physiological concentration of OHP on the cellular electrical properties of differentiated F-11 cells. For comparison, some experiments were reproduced on embryonic and adult rat DRG neurons in order to validate the differentiated F-11 cells as an adequate *in vitro* model for the study of OIPN.

In the following pages, the technical aspects of our experiments will be described in detail (Materials and methods). In the results section, we will show the collected data regarding the effects of OHP on the cellular electrical properties and its interactions with voltage-dependent ion channels in the proposed three models of sensory neurons: differentiated F-11 cell, embryonic and adult rat DRG neuron cultures. Then, our findings will be discussed in comparison with the wide spectrum of mechanisms reported in literature for the onset of acute OIPN. Finally, future perspectives will be proposed in the last section.

2. MATERIALS AND METHODS

2.1 Cell cultures

The neurotoxic effects of OHP were studied on three different *in vitro* models. In particular, our experiments were performed on differentiated F-11 cells and primary sensory neurons derived from the enzymatic and mechanical dissociation of embryonic and adult rat dorsal root ganglia (DRGs).

2.1.1 F-11 cell line

The F-11 cell line is a somatic hybrid produced by fusion of embryonic rat dorsal root ganglion neurons and mouse neuroblastoma cells N18TG-2 (Platika et al., 1985).

F-11 cells were seeded at 60 000 cells/35 mm dish and routinely cultured in Dulbecco's modified Eagle's medium (Sigma-Aldrich, St. Louis, MO, USA), 10% of fetal bovine serum (Sigma-Aldrich), 2mM glutamine (Sigma-Aldrich) and incubated at 37°C in a humidified atmosphere with 5% CO_2. In order to induce the differentiation process towards neuronal commitment, F-11 cells were cultured for 14 days in serum starvation (1% of fetal bovine serum). After 14 days in this conditions, the obtained differentiated cultures were treated with OHP 7.5 µM for 24h-48h or with CDDP 15 µM for 24h. During our experiments, non-treated cultures were used as controls.

2.1.2 Primary cultures of DRG neurons

Primary cultures of embryonic or adult rat sensory neurons were used to validate the results obtained on differentiated F-11 cells. All the procedures conducted on animals were carried out under anesthesia in

conformity with the institutional guidelines in compliance with national (D. L.vo 26/2014) and international laws and policies (European Union directive 2010/63/EU).

Rat embryonic DRG neurons

DRG from 15 day old embryonic Sprague-Dawley rats (Envigo, Udine, Italy) were aseptically removed and collected in 15 ml tubes filled with Leibovitz-15 medium (Invitrogen, Carlsbad, CA). DRGs were then centrifuged at 1500 rpm for 10 minutes at 4°C and the supernatant was discarded. The ganglia were dissociated by incubation with trypsin 0.25% for 30 minutes at 37°C. The digestion was blocked by removing trypsin after centrifugation at 1500 rpm for 10 minutes at 4°C. Next, 500 µl of AN_2 medium composed by MEM (Invitrogen, Carlsbad, CA), plus 15% Calf Bovine Serum (Hyclone, Logan, UT, USA), 50 µg/ml ascorbic acid (Sigma-Aldrich), 1.4 mM L-glutamine (Invitrogen), 0.6% glucose (Sigma-Aldrich) supplemented with 5 ng/ml NGF (Invitrogen) was added and the ganglia were mechanically disrupted using a Pasteur pipette. Post-mitotic neurons were then plated in a single drop (80 µl) onto 35mm dishes previously coated with rat tail collagen, incubated at 37°C in a humidified atmosphere with 5% CO_2 and added with fresh medium after 2h. In order to obtain enriched neuronal cultures, after 24h neurons were treated for 5 days with AN_2 medium supplemented with 5 ng/ml NGF and 10^{-5} M 2′-Deoxy-5-fluorouridine (FuDR, Sigma Aldrich) to remove satellite cells, which remain as contaminants in a percentage lower than 5% at the end of the treatment (Scuteri et al., 2009). Neurons were then incubated with AN_2 medium with 5 ng/ml

NGF for 24 h, and the next day were treated with OHP for 24 or 48 h. Untreated cultures were used as control.

Four independent experiments were performed on embryonic DRG neurons.

Adult rat DRG neurons

DRG neurons were obtained from 12-14 week male Sprague Dawly rats (350-400 g, Envigo).

Under deep anesthesia, rats were bleed by aorta blood sampling and the spinal cord was exposed in order to allow a complete DRG pool harvest. The collected ganglia were maintained in a culture dish containing 1,8 ml of F12 medium. After cleaning the samples from nerves and blood, DRGs were transferred in a 2 ml tube containing 1.8 ml of F12 medium which have been previously incubated to reach the right pH. DRGs were then added with DNase I (Sigma-Aldrich) and collagenase 0.125% (Sigma Aldrich) and incubated at room temperature for 2 h to facilitate enzymatic digestion. This latter was then stopped by removing the medium and adding 1 ml of fresh F12 medium. Ganglia were then centrifuged, the supernatant discarded and the DRGs were mechanically disrupted using a pipette. Subsequently, the cell suspension was transferred to the BSA gradient and centrifuged at room temperature at 1000 rpm for 6 minutes without brake. After centrifugation, the second and first phase were discarded while the pelletted neurons were resuspended in 1 ml of fresh Bottenstein and Stato's (BS) medium. To remove all the bovine serum albumin (BSA) remains, the cells were then centrifuged 2 times at 1000 rpm for 6 minutes at room temperature with brake. Finally, DRG neurons were pleated in a single drop (100 µl) on previously poly-

lysine coated culture dishes in BS medium and incubated at 37°C in a humidified atmosphere with 5% CO_2. After 30 minutes from seeding, neuronal cultures were added with fresh medium and after 24 h were treated with FuDR (Sigma Aldrich) for 72 h to remove proliferating cells (glial cells and fibroblasts). The drug was then washed out for 24 h to avoid any interference between FuDR and the drugs under exam. The DRG neuronal cultures obtained with this procedure were treated for 24h with OHP. Untreated cultures were used as controls.

All the analysis on adult DRGs neurons were performed in two independent experiments.

2.2 Drug treatments

***Cisplatin* (CDDP)**

Cis-Diammineplatinum(II) dichloride (Sigma Aldrich) was dissolved in physiological solution 1 mg/ml to prepare a stock solution (3.33 mM) and then diluted with our medium to reach the working concentration of 15 µM. CDDP was freshly prepared before each experiment in type I glass vials.

***Oxaliplatin* (OHP)**

Oxalato(trans-$_L$-1,2-diaminocyclohexane)platinum (Sigma Aldrich) was dissolved in water 5 mg/ml to obtain a stock solution 12.5 mM stored at -20°C until use. The stock solution was then diluted in fresh medium to obtain the treatment solution of 7.5 µM.

2.3 Patch-clamp recordings

All electrophysiological recordings were performed in the whole-cell configuration of the patch-clamp technique, in current-clamp or in voltage-clamp mode.

From the experiments conducted in current-clamp mode, we extracted information about the effects of OHP on the resting membrane potential (V_{Rest}) and on spontaneous and evoked action potential (AP) features. In voltage-clamp mode we studied the interactions of OHP with sodium and potassium channels and, therefore, the current densities and their biophysical properties.

Micropipettes (2–3 MΩ) were pulled from borosilicate capillaries with a P-97 Flaming/Brown Micropipette Puller (Sutter Instrument Co., Novato, CA). The ground electrode was a bridge of 3% agar. During experiments with F-11 cells cell capacitance and series resistance were compensated up to approximately 85-90% before each voltage-clamp protocol run. Cells were inspected with an inverted microscope (Eclipse TS100, Nikon Corporation, Tokyo, Japan). They were perfused at ~700 µl/min and drugs were applied with an RSC-160 Rapid Solution Changer (Bio-Logic Science Instruments, Claix, France). All recordings were collected, at room temperature, by the pClamp8 software and the MultiClamp 700A amplifier (Axon Instrument).

The stimulation protocols used for all the electrophysiological recordings are described in details in the results section.

2.3.1 Experimental solutions

During the experiments aimed to study voltage-dependent sodium and potassium channels, the standard extracellular solution contained (mM): NaCl 135, KCl 2 $CaCl_2$ 2, $MgCl_2$ 2, HEPES 10, glucose 5, pH 7.4. In some of these experiments, tetrodotoxin (TTX, Sigma Aldrich, 0.3 µM or 1 µM final concentrations) was added to block the voltage-dependent Na^+ current.

The standard pipette solution was composed as follows (mM): potassium aspartate 130, NaCl 10, $MgCl_2$ 2, $CaCl_2$ 1.3, EGTA 10, HEPES 10, pH 7.3.

The biophysical properties of voltage-dependent sodium channels were investigated using a pipette solution containing (mM): NaCl 5, $MgCl_2$ 2, CsF 105, CsCl 27, EGTA 10, HEPES 10. In this way, the substitution of potassium ions with cesium ions allowed us to completely abolish potassium currents.

In order to study ERG potassium channels, their currents were recorded using an external solution containing a high potassium concentration (mM): NaCl 95, KCl 40, $CaCl_2$ 2, $MgCl_2$ 2, hepes 10, glucose 5, pH 7.29. This expedient shifted the K^+ equilibrium potential (E_K= -30mM), allowing us to obtain larger inward currents at negative Vm. During the investigations on ERG inactivation properties, a specific blocker was added at saturating concentration (WAY123.398, 1 µM) to isolate spurious potassium currents and subtract them during data analysis.

TTX and WAY123.398 were bath applied.

2.3.2 Analysis of patch-clamp data

For the analysis, Origin 9.0 (Microcal Inc., Northampton, MA) and Excel were routinely used. In the captions, n refers to the number of tested cells. Before statistical analysis the Shapiro-Wilk test was used to assess the normal distribution or our data. Unless otherwise indicated, statistical significance was assessed with one-way analysis of variance (ANOVA) at the indicated level of significance (p), followed by the Tukey post hoc test, the Student's *t*-test or the χ^2 test. Mann-Whitney non-parametric U test was used to evaluate data not showing a normal distribution. One-way ANOVA was used for multiple comparisons while the Student's *t*-test and Mann-Whitney non-parametric U test were used to compare pairs of data samples. The results are indicated as mean values ± SEM.

3. RESULTS

In order to study the acute effects of OHP on the cellular electrical properties and its eventual interaction with voltage-dependent ion channels, electrophysiological investigations were conducted on F-11 cells, a somatic cell hybrid of rat embryonic dorsal root ganglia (DRG) and mouse neuroblastoma cell line N18TG-2, differentiated toward a neuronal commitment. F-11 cells represent a good cellular model of DRG because they resemble morphologically mature neurons and they can form networks with spontaneous electrical activity, which indicates their ability to express voltage-gated ion channels and ligand-gated receptors, and release neurotransmitters. Moreover, the employment of a neuron-like immortalized cell line spared us the need of animal sacrifices to collect *ex-vivo* samples and the statistical variability deriving from the cellular heterogeneity typical of primary cultures.

CDDP is an anti-cancer drug, which was the first developed molecule among the platinum compound class. Clinical data show that CDDP administration does not produce the acute symptoms of peripheral neurotoxicity described for around 90% of the patients treated with OHP (Lehky et al., 2004). For this reason, we decided to use this compound as reference to verify that a possible effect on the electrophysiological properties of the tested cells would be correlated with the interaction with OHP.

During our experiments, we treated our cultures with OHP 7.5 µM, a lower concentration compared to the usual doses found in literature (Adelsberger et al., 2000; Webster et al., 2005; Kagiava et al., 2008; Wu et al., 2009). This concentration was chosen because preliminary

assays performed in our laboratory on embryonic rat DRG neuron cultures incubated with OHP 7.5 µM showed a marked effect on the neurite elongation ability. In fact, the 24 h-long treatment with OHP reduced the axon growth by 13.68 ± 2.55% compared to non treated cells, while incubation of our cultures with the drug for 48 h produced a reduction of 52.15 ± 3.88%. The same experiment conducted after 24 h incubation with CDDP 15 µM showed a 25% decrease for this parameter. Considering that the universally accepted threshold for the neurotoxicity is set at 50% for the neurite elongation test, we decided not to exceed the concentrations of 7.5 µM for OHP and 15 µM for CDDP.

Differently from other studies found in literature, which focused their attention on individual aspects of the electrophysiological cellular response to OHP administration (Adelsberger et al., 2000; Grolleau et al., 2001; Webster et al., 2005; Benoit et al., 2006; Kagiava et al., 2008), we chose to perform a complete characterization of the electrical properties of the tested cells, evaluating the effects of the compound on the resting potential (V_{Rest}) and the action potential (AP) characteristics and on the voltage-dependent sodium and potassium channel properties that sustain neuronal electrical activity.

Finally, in order to validate the results collected in the differentiated F-11 cellular model, our experiments were reproduced on DRG neuron primary cultures deriving from the enzymatic and mechanical dissociation of dissected embryonic and adult DRGs.

3.1 Differentiated F-11 cells

3.1.1 Effects of OHP on the electrical activity

By the patch-clamp technique, in the current-clamp mode, we tested the effect of OHP on the electrical properties of differentiated F-11 cells in culture. In particular, our attention was focused on possible alterations of the V_{Rest}, of the spontaneous electrical activity and of the induced AP properties.

Effects on V_{Rest} produced by platinum analogues

Figure 1 shows a progressive and significant depolarization of V_{Rest} in response to 24 h and 48 h incubation of the cultures with OHP. On the contrary, 24 h long treatments with CDDP did not produce any alteration of this parameter.

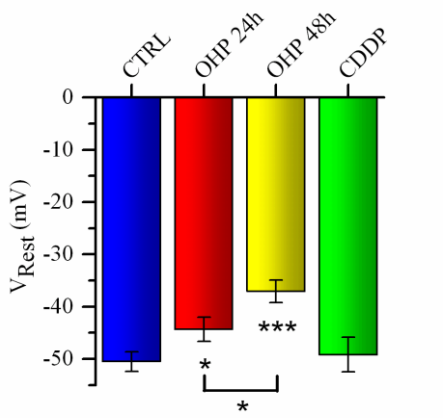

Figure 1. Effects of the treatments with platinum compounds on the resting potential (V_{Rest}) of differentiated F-11 cells. The histogram shows that the exposure to oxaliplatin (OHP) produced an increasing and significant depolarization of the membrane in the tested cells while cisplatin (CDDP) exerted no measurable effects. The average values were: -50 ± 2 mV in non treated cells (n=40), -44 ± 2 mV in the cells treated with OHP for 24 h (n=25), -37 ± 2 mV in the cells treated with OHP for 48 h (n=20) and -49 ± 3 mV in the cells treated with CDDP for 24 h (n=28). Statistical evaluations were obtained using the one-way analysis of variance

(ANOVA), followed by the Tukey post hoc test. *p<0.05 for OHP 24 h *vs* CTRL and OHP 48 h *vs* OHP 24 h; ***p<0.0001 for OHP 48 h *vs* CTRL.

Effects of platinum drugs on the spontaneous electrical activity

Another aspect which has been evaluated was the presence of spontaneous APs during our recordings. This type of activity was made possible by the fact that the tested F-11 cells have been previously addressed toward neuronal commitment and this process induced them to form neuronal networks after 14 days in vitro. From our data, it emerges that the treatment with OHP for 48 h led to a significant reduction of the number of cells showing spontaneous activity (**Figure 2**). On the contrary, the incubation with CDDP did not influence the ability to spontaneously generate APs.

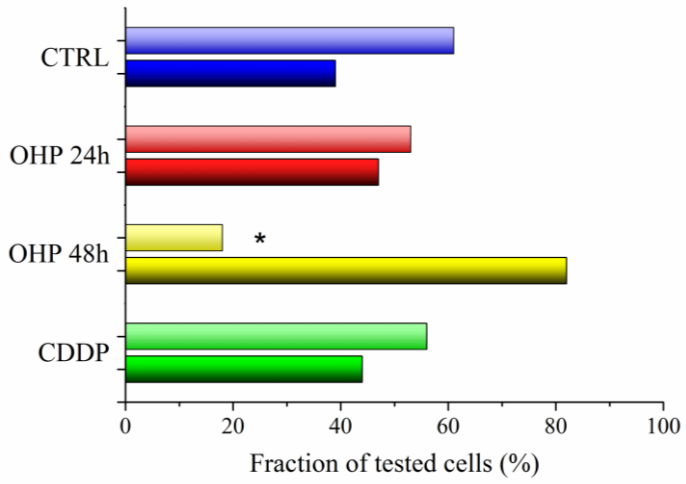

Figure 2. Effect of platinum compounds on the cell ability to generate spontaneous action potentials (APs). The fraction of cells in which the presence of spontaneous APs has been observed was: 61% in control cells (n=36), 53 % in the cells treated with oxaliplatin (OHP) for 24 h (n=19), 18% in the cells treated with OHP for 48 h (n=11) and 56% in the cells treated with cisplatin (CDDP) for 24 h (n=9). Light bars represent cells which showed spontaneous APs, while dark bars represent the fraction of cells without this type of activity. * p= 0.013 OHP 48h *vs* CTRL, χ^2 test).

Influences of platinum agents on induced APs

The induced APs were studied using a stimulation protocol under conditioning hyperpolarization at -75/-80 mV; the protocol consisted in the injection of increasing steps of depolarizing current, with a duration of one second, in order to make the cell membrane reach the threshold for AP generation (**Figure 3A**).

In each tested cell, the firing frequency was calculated considering the highest number of evoked APs ≥ 0 mV that could be generated during depolarizing current injection. After 24 h the cells treated with OHP showed a non significant reduction of the firing frequency of the APs. However, the longer treatment (48 h) produced a significant decrease of the same parameter. Data collected on cultures treated with CDDP 15 µM for 24 h showed an even more considerable reduction of the firing frequency (**Figure 3B-C**).

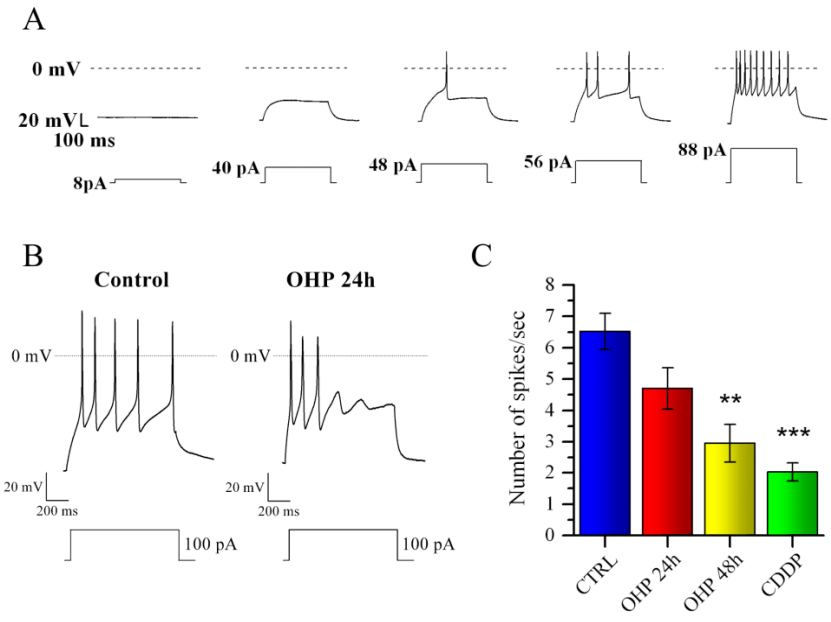

Figure 3. Effects of platinum analogues on evoked firing frequency. A. Representation of a typical stimulation protocol in current-clamp mode. The

electrical response of the cell, in terms of membrane potential variation, is also visible in the upper part of the panel. **B.** Representative traces of induced electrical activity of F-11 cells in the absence or in the presence of oxaliplatin (OHP) treatment for 24 h. **C.** The firing frequency was calculated considering the highest number of evoked APs ≥ 0 mV that could be generated during depolarizing current injection. The histogram shows that the treatment with OHP determined a progressive reduction of the APs frequency. This effect became significant in the cells incubated with OHP for 48 h. A further decrease has been observed in the F-11 cells treated with cisplatin (CDDP) for 24 h. The average collected values were: 6.52 ± 0.58 Hz in non-treated control cells (n=40), 4.7 ± 0.66 Hz in cells incubated with OHP for 24 h (n=24), 2.95 ± 0.60 Hz in cells treated with OHP for 48 h (n=19) and 2.03 ± 0.30 Hz in cells incubated with CDDP for 24 h (n=32). ** p< 0.01 for OHP 48 h *vs* CTRL; *** p<0.001 for CDDP 24 h *vs* CTRL (Mann-Whitney non-parametric test).

Another feature evaluated during our studies was the AP amplitude, calculated as the difference between the peak voltage reached by the AP and the V_{Rest} (**Figure 4A**). Treatment with OHP for 24 h did not alter the amplitude of APs while CDDP administration significantly increase the same parameter (**Figure 4B**).

During data analysis, we also studied another parameter describing the AP, i.e. the duration. This feature was evaluated on the first AP evoked by injected threshold current. This choice was made in order to exclude the influence of the adaptation phenomenon, which may occur during trains of APs. In this condition, the duration was calculated as the spike width measured at intersection between the AP shape and the axis at 0 mV and was expressed in ms (**Figure 4A**). **Figure 4C** shows that both treatments with OHP did not produce any effect on the duration of the APs. In contrast, CDDP administration was able to increase this parameter.

Moreover, we analyzed the effects of OHP treatment on the after-hyperpolarization that is calculated as the lowest value reached by the Vm at the end of the AP repolarization. OHP treated cells showed a

shift of this feature towards more depolarized values compared to control (**Figure 4D**). Similarly, the incubation with CDDP produced the same effect on this feature.

Finally, we measured the time course of the AP repolarization. This was described by the tau parameter (τ, expressed in ms) that was determined from single exponential fit on the voltage increase from the lowest value of the after-hyperpolarization to V_{Rest}. The function used during the fitting procedure was:

$$f(t) = Ae^{-t/\tau} + C$$

Where A is the amplitude of the repolarization, τ is the time constant and C is the constant y-offset.

Figure 4F shows that the incubation with OHP for 24 h decrease the average τ values.

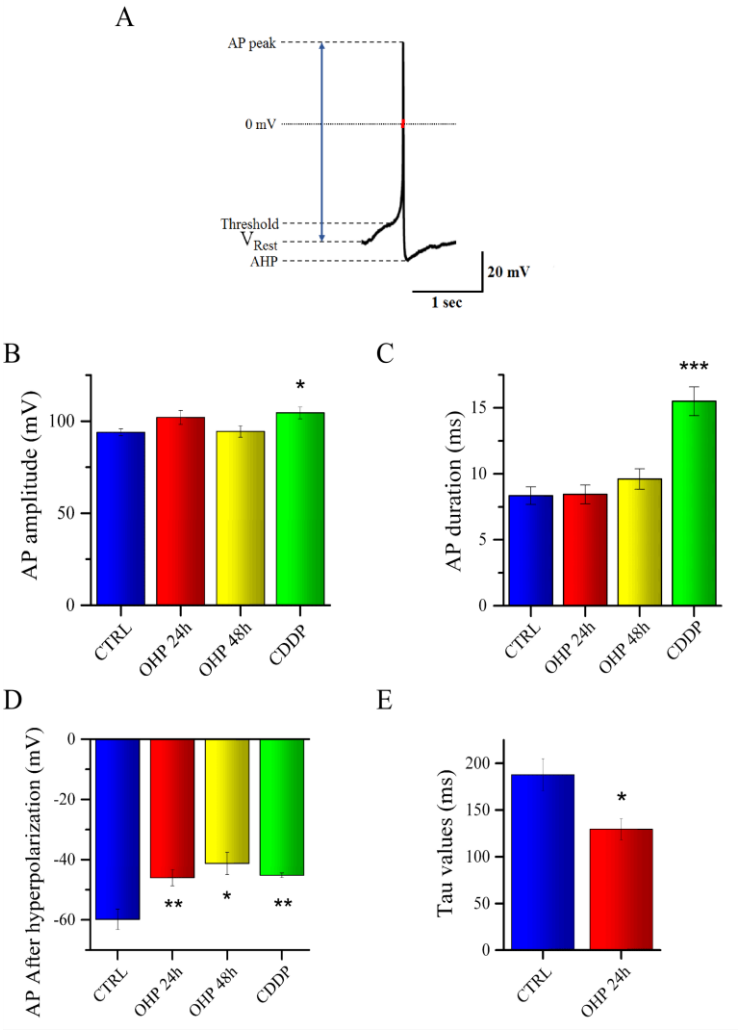

Figure 4. Effects of platinum drugs on action potential (AP) characteristics. A. Graphical representation of a single AP. This figure shows how the AP features were calculated; red horizontal bar represents the AP duration while the vertical blue bar indicate the AP amplitude. **B.** OHP administration did not produce any effect on the AP amplitude. In contrast, CDDP administration induced an increase of the same parameter. The average values were: 93.92 ± 1.85 mV for control non-treated cells (n=40), 102.04 ± 3.75 mV in cells incubated with OHP for 24 h (n=24), 94.4 ± 3.1 mV for OHP 48 h incubated cells (n=18), and 104.54 ± 3.17 mV for CDDP incubated cells (n=24). *P< 0.05 for CDDP *vs* CTRL (ANOVA, followed by the Tukey post hoc test). **C.** OHP did not affect the AP duration, whereas the incubation with CDDP induced a significant increase of the same feature. The observed mean values were: 8.35 ± 0.65 ms in control cells (n=40), 8.45 ± 0.71 ms in cells treated

with OHP for 24 h (n=24), 9.61 ± 0.77 ms for OHP 48 h treated cells (n=18) and 15.5 ± 1.09 ms in CDDP treated cells (n=24). *** p<0.001 CDDP *vs* CTRL (Mann-Whitney test). **D.** The incubation with platinum analogues induced a shift of membrane after-hyperpolarization potential towards more depolarized values. The mean observed values were: -59.83 ± 3.38 mV for CTRL cells (n=6), -46 ± 2.7 mV for 24 h OHP treated cells (n=6), -41.25 ± 3.57 mV for 48 h OHP treated (n=5) and -45.2 ± 0.8 for CDDP treated cells (n=5). ** p< 0.01 for CTRL *vs* OHP 24 and CDDP, *p<0.05 OHP 48 h *vs* CTRL (ANOVA, followed by the Tukey post hoc test). **E.** The histogram shows that incubation with OHP reduce the value of the τ parameter. The average values were: 187.66 ± 17.15 ms for non-treated cells (n=6), 129.33 ± 11.22 ms for OHP 24 h treated cells (n=6). * p< 0.05 for OHP 24 h cells *vs* CTRL (Student's *t*-test).

3.1.2 OHP affected the gating properties of voltage-dependent sodium and potassium channels

To better evaluate the effects produced by the incubation with OHP on the overall electrical activity of differentiated F-11 cells, we decided to investigate the electrophysiological aspects at the base of the variations observed on the V_{Rest} and on the spontaneous and induced APs. For this purpose we determined the effects produced by our compounds on the voltage-dependent sodium and potassium channels, which sustain the neuronal electrical activity.

Effects of platinum analogues on the current densities of sodium and potassium delayed-rectifier

Sodium and potassium currents were studied in voltage-clamp mode by applying the following protocol: starting from an holding potential of -60 mV, the cells were preconditioned at -100 mV for 500 ms and then tested with depolarizing steps with an increasing amplitude of 10 mV (from -80 mV to +60 mV) and lasting 100 ms (**figure 5A**).

The recorded currents had two principal components: the former, more rapid and inward, due to the voltage-dependent sodium channel opening, and the second, slower and outward, which was produced by the opening of voltage-dependent potassium channels and was consistent with delayed rectifier current profile (**figure 5B**).

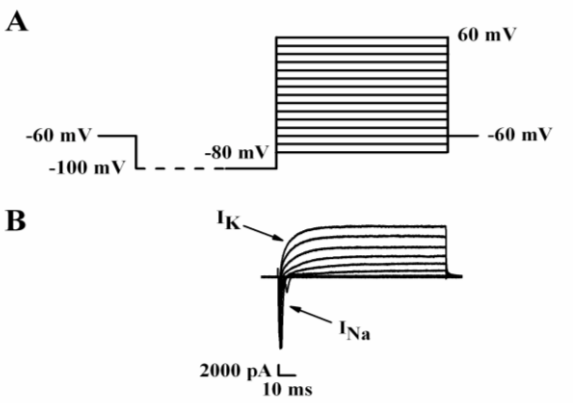

Figure 5. Voltage-dependent sodium and potassium currents recorded in differentiated F-11 cells by patch-clamp technique in the whole-cell configuration. A. Graphical representation of the stimulation protocol applied to the cell in voltage-clamp mode. **B.** Representative trace obtained by the application of the protocol described in the above panel (sodium current, I_{Na}, and potassium current, I_K).

The protocol described above was reproduced on every tested cell during the administration of a saturating concentration of tetrodotoxin (TTX, 1 µM), a highly selective inhibitor of voltage-dependent sodium channels. We also used a lower concentration (0.3 µM) in order to reveal the possible presence of a TTX-resistant component of the voltage-dependent sodium current. By completely blocking the current flowing through voltage-dependent sodium channels it was possible to isolate the outward current resulting from the sole opening of voltage-dependent delayed rectifier potassium channels. During data analysis, the TTX-sensitive Na^+ current was revealed by subtracting the K^+ current from the total current. Finally, for each tested cell, the sodium and potassium current densities were calculated as the ratio between the peak I_{Na} current or the steady-state I_K current and the measured membrane capacitance (pA/pF). Our data showed that treating our cultures with OHP for 24 h and 48 h significantly

increased the voltage-dependent sodium current density. On the contrary, the administration of CDDP for 24 h strongly reduced it (**Figure 6**). Data collected with the use of an external solution containing 1 µM TTX were in line with the one obtained using the lower concentration of this drug (TTX 0.3 µM).

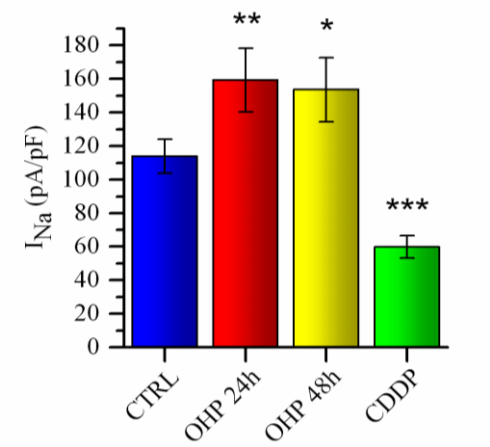

Figure 6. Effect of platinum compounds on voltage-dependent sodium current density. Whole-cell currents were elicited by the protocol shown in **Figure 5A** under control conditions and during oxaliplatin (OHP) or cisplatin (CDDP) cell treatment. Incubation with OHP determined an increase in sodium current densities. However, the incubation with 15 µM CDDP for 24 h produced a strong reduction of the investigated feature. The mean observed values were: 114 ± 10.21 pA/pF in non-treated cells (n=37), 159.27 ± 18.98 pA/pF in the cells treated with OHP for 24 h (n=25), 153.63 ± 19.09 pA/pF in the cells treated for 48 h (n=20) and 59.68 ± 6.70 pA/pF in the cells treated with CDDP for 24 h (n=24). ** $p<0.01$ for OHP 24 h vs CTRL; * $p<0.05$ for OHP 48 h *vs* CTRL; *** $p<0.001$ for CDDP 24 h *vs* CTRL (Mann-Whitney test).

Concerning the delayed rectifier potassium channels, our data show that treatment with platinum compounds determined a reduction of the current density which was statistically significant only in the cells treated with CDDP for 24 h (**Figure 7**).

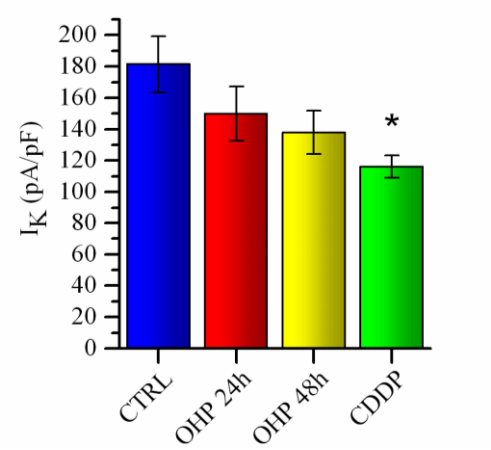

Figure 7. Effects of platinum based antineoplastc drug on potassium current density. Oxaliplatin (OHP) application produced a progressive but not significant decrease of potassium current density. The 24 h long treatment with cisplatin (CDDP) determined a significant reduction of the same feature. The observed average values were: 181.42 ± 17.89 pA/pF in non-treated control cells (n=37), 149.86 ± 17.25 pA/pF in the cells cultured 24 h in the presence of OHP (n=25), 137.94 ± 13.77 pA/pF in the cells treated for 48 h with OHP (n=20) and 116.11 ± 7.11 pA/pF in CDDP-treated cells (n=27). * $p<0.05$ for CDDP 24 h *vs* CTRL (Mann-Whitney test).

Alteration produced by platinum drugs on ERG current density

Since differentiated F-11 cells also express ERG (*ether-à-go-go related* gene) channels, our investigations were then focused on the possible effects of OHP on these channels.

The ERG current density was studied in the presence of an external solution containing a high concentration of potassium ions (40 mM) in order to shift the potassium equilibrium potential E_k; in this way we were able to study the current flowing through ERG channels as inward tail current at -120 mV. Moreover the ERG single-channel conductance increases by raising the extracellular concentration of potassium ions $[K^+]_o$. Therefore, our experimental condition increased the recorded ERG currents.

This variation of the ionic composition of the experimental solution allowed us to amplify and isolate this component from the other potassium currents (delayed rectifier). The experiments were conducted in voltage-clamp mode using a stimulation protocol which started from a holding potential of -60 mV, followed by the application of preconditioning voltage steps with a duration of 15 seconds and amplitudes from +20 mV to -80 mV, and ended with a test potential at -120 mV (**Figure 8A**). While membrane depolarization increases the fraction of inactivated ERG channels, the rapid transition to a very negative test potential removes the inactivation, generating a current ("tail current") which is proportional to the initial depolarization. For instance, since the inactivated fraction is maximal at +20 mV, the transition to -120 mV produces the maximal observable tail current (**Figure 8B**).

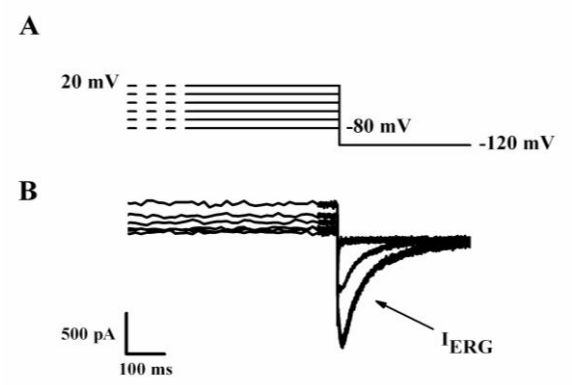

Figure 8. ERG current recorded from differentiated F-11 cells. A. Stimulation protocol in voltage-clamp mode used during our experiments in order to study ERG current (I_{ERG}) activation. **B.** Representative trace recorded using the protocol represented in the above panel.

In each tested cell, ERG current density was calculated as the ratio between the amplitude of the maximum peak current and the membrane capacitance (pA/pF).

Data analysis showed that the incubation with OHP for 24 h significantly reduced ERG current density while the longer treatment (48 h) did not produce significant effects even though a decreasing tendency was observed. The administration of CDDP significantly reduced the same feature (**Figure 9**).

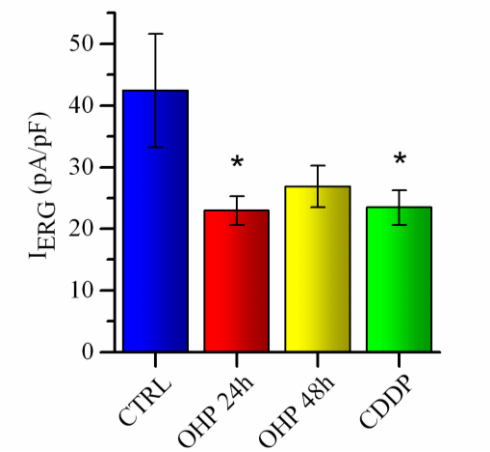

Figure 9. Effects of platinum compounds on ERG current density. Whole-cell currents were elicited by voltage protocol shown in **Figure 7A** under control conditions and in the presence of oxaliplatin (OHP) or cisplatin (CDDP). The histogram shows that the administration of OHP and CDDP for 24 h produced a significant decrease of the ERG current density. On the contrary, the treatment with OHP for 48 h did not produce a significant effect. The mean values were: 42.44 ± 9.18 pA/pF in non-treated cells (n=8), 22.96 ± 2.37 pA/pF in the cells incubated with OHP for 24 h (n=16), 26.90 ± 3.34 pA/pF in the cells treated with OHP for 48 h (n=11) and 23.45 ± 2.84 pA/pF in the cells treated with CDDP for 24 h (n=14). * $p<0.05$ for OHP 24 h *vs* CTRL, * $p<0.05$ for CDDP *vs* CTRL (ANOVA, followed by the Tukey post hoc test).

3.1.3 Effects of platinum drugs on the biophysical properties of sodium and ERG potassium channels

To better understand the causes of the observed variations in sodium and ERG current densities, we investigated the biophysical properties of these channels constructing the activation and inactivation curves for cells treated with OHP for 24 h.

Effects of platinum analogues on voltage-dependent sodium channel activation and inactivation curves

The activation curve is a function which describes the probability to find voltage-dependent channels in the open state in correspondence to a given Vm, at the steady-state. The activation of sodium channels was studied using the voltage protocol formerly described for the investigation of sodium and potassium current densities and using an internal solution containing 105 mM cesium fluoride and 27 mM cesium chloride (**Figure 5A**). Cesium ions present the same single positive charge of potassium ions but also a larger atomic diameter which prevents them from flowing through the selective pores of voltage-dependent potassium channels. For these reasons, the complete substitution of potassium ions with cesium ions did not alter the osmotic equilibrium of the tested cells and the overall electromotive force and, at the same time, this expedient abolished the ionic currents flowing through opened voltage-dependent potassium channels.

Also in this case, the protocol was repeated in the presence of 1 μM TTX in order to block sodium currents. During data analysis, the two recorded traces were subtracted therefore revealing the current produced by the sole activation of the TTX-sensitive voltage-

dependent sodium channels. The activation curve was built reporting the conductance values (g) of sodium channels normalized to the g obtained in response to a depolarizing voltage step of sufficient magnitude to elicit maximum peak Na^+ current (g_{max}).

The conductance values were calculated with the equation:

$$g = \frac{I}{(V_m - E_{Na})}$$

Where I is the amplitude of the recorded current, V_m is the imposed membrane potential and E_{Na} is the Nerst potential for sodium ions that was measured through the application of protocol in **Figure 10A**. The g_{max} value was calculated using the following equation:

$$g_{max} = \frac{I_{max}}{(V_m - E_{Na})}$$

Data for each cell (**Figure 10A**) were fitted to a Boltzmann distribution equation of the following form:

$$\frac{g}{g_{max}} = \frac{1}{1 + e^{\frac{V_m - V_{1/2}}{k}}}$$

where g_{max} is the maximum g, $V_{1/2}$ is the potential at which channel activation is half-maximal, and k is the slope of the curve.

Collected data showed that 24 h treatment with OHP determined a significant (p=0.011) shift of voltage-dependent sodium channel activation curve towards more negative membrane potentials compared to non treated cells. The observed mean values for $V_{1/2}$ were -21.91 ± 0.47 mV in control cells and -30.71 ± 1.7 mV in the cells incubated with OHP. The slope factors were 6.18 ± 0.41 mV and 4.70

± 0.72 mV respectively (**Figure 10B**) and were not significantly different. In contrast, CDDP administration induced a significant shift of voltage-dependent sodium channel activation curve towards more positive membrane potentials compared to control condition (p=0.009). The mean value for $V_{1/2}$ of CDDP treated cells was -4.02 ± 0.33 mV with a k slope factor of 6.85 ± 0.29 mV.

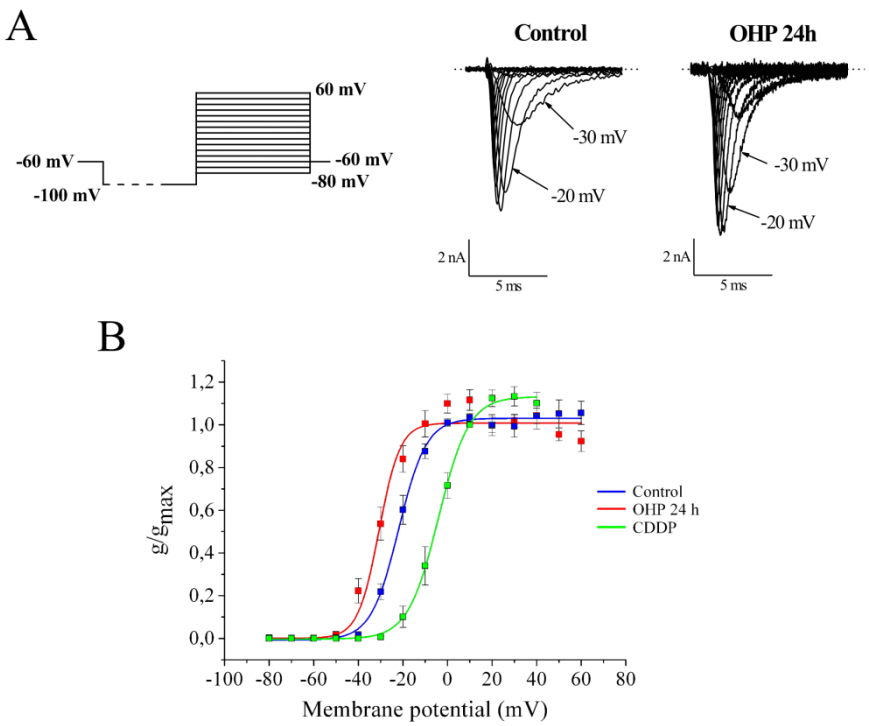

Figure 10. Effects of platinum compounds on the activation curves of voltage-dependent sodium channels. **A.** The panel represents on the left the stimulation protocol used during these experiments and, on the right, current traces recorded in control conditions or in presence of oxaliplatin (OHP) for 24 h. **B.** Activation curves of voltage-dependent sodium channels in a series of experiments conducted in control condition (in blue, n= 5) or in the presence of OHP for 24 h (in red, n=6) or CDDP (in green, n=4). OHP administration significantly shifted the activation curve of voltage-dependent sodium channels towards more negative values. On the other hand, the incubation with CDDP significantly shifted the activation curve of voltage-dependent sodium channels towards more positive values. The mean values for $V_{1/2}$ were -21.91 ± 0.47 mV for non-treated cells, -30.71 ± 1.7 mV for OHP

treated cells and -4.02 ± 0.33 mV for cells incubated with CDDP. The slope factors were 6.18 ± 0.41 mV, 4.70 ± 0.72 mV and 6.85 ± 0.29 mV respectively. $p<0.05$ for OHP *vs* CTRL, $p<0.01$ for CDDP *vs* CTRL (ANOVA, followed by the Tukey post hoc test).

To study the inactivation process of sodium channels we used a stimulation protocol which started from a holding potential of -80 mV, continued with the application of conditioning steps with an increasing amplitude of 15 mV (from -105 mV to 0 mV) and a duration of 600 ms and ended with a test at -10 mV lasting 65 ms. At -105 mV, the inactivation is completely removed from voltage-dependent sodium channels and, therefore, all the channels are available but in the closed state. From this Vm, a rapid transition to -10 mV, the potential which elicits the activation of the highest percentage of channels, makes the channels open very quickly, thus producing the maximal current. As the conditioning potential moves to more positive values, the fraction of channels in the inactivated state progressively increases reducing the current produced at -10 mV. For this reason, since at 0 mV the voltage-dependent sodium channels are completely inactivated, the test at -10 mV does not produce any detectable current (**Figure 11A and Figure 11B**).

The inactivation curve was calculated plotting the amplitude values of the recorded currents measured at the peak (I) and normalized on the amplitude of the maximal current (I_{max}) as a function of the imposed membrane potential.

The values obtained by the average of 7 control cells and 8 cells in 24 h OHP were interpolated by a Boltzmann function with equation:

$$\frac{I}{I_{max}} = \frac{1}{1 + e^{\frac{V_{1/2} - V_{pre}}{k}}}$$

where I_{max} is the maximum sodium current elicited after the most hyperpolarized preconditioning potential, the Vpre is the preconditioning potential, $V_{1/2}$ is the potential at which inactivation is half-maximal, and *k* is the slope factor.

The analysis of the collected data showed that treating the cultures with OHP for 24 h determined a slight shift of the inactivation curve for voltage-dependent sodium channels towards more negative values compared to non-treated control cells. In contrast CDDP treatment induced a shift of the inactivation curve towards more positive membrane potential values. The mean values of $V_{1/2}$ were: -68.12 ± 2.12 mV for non treated cells, -72.09 mV for cells incubated with OHP (p=0.005) and -58.21 ± 0.72 mV for CDDP treated cells (**Figure 11C**). *K* values were: 5.12 ± 0.98, 5.25 ± 0.26 and 7.79 ± 0.61 mV respectively.

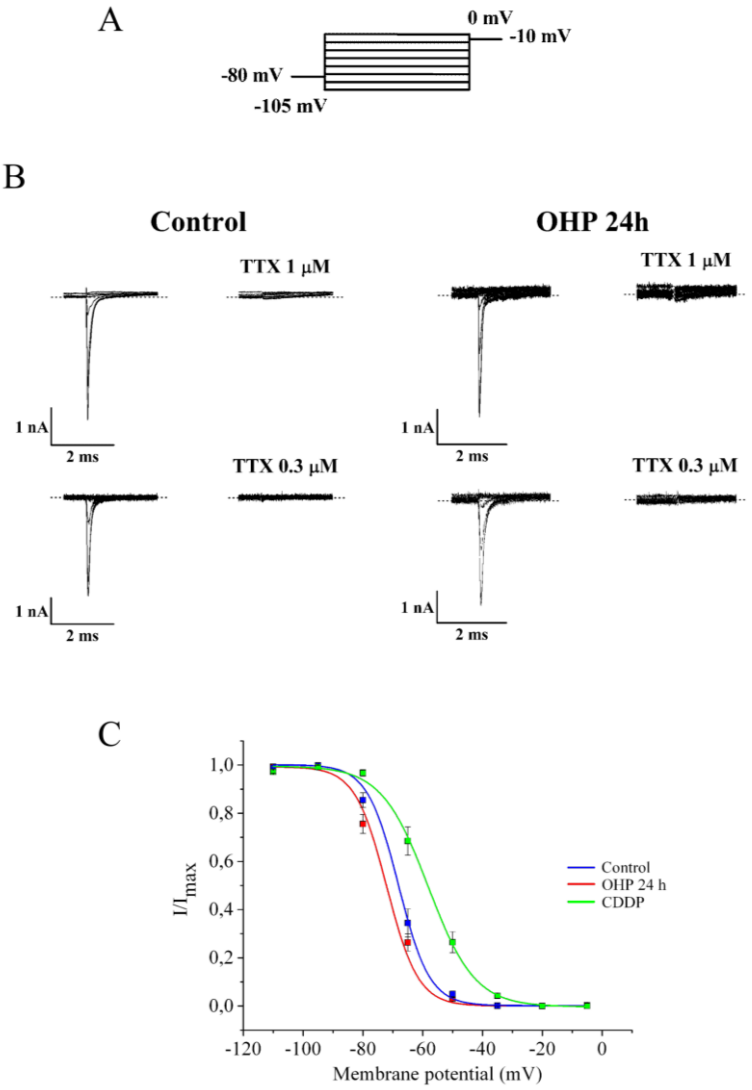

Figure 11. Effects of platinum-based drugs incubation on the inactivation curves of voltage-dependent sodium channels. **A.** Graphical representation of the stimulation protocol in voltage-clamp mode applied to study the inactivation process of voltage-gated sodium channels. **B.** Traces recorded in the presence or in the absence of TTX 1µM or 0.3 µM in control condition or after 24 h treatment with OHP. **C.** Inactivation curves of voltage-dependent sodium channels in a series of experiments conducted in the absence (in blue, n=7), in the presence of oxaliplatin (OHP) for 24 h (in red, n=8) or cisplatin (CDDP) for 24 h (in green, n=6). While CDDP treatment shift the inactivation curve towards more positive values, OHP administration for 24 h shifted the inactivation curve of voltage dependent sodium channels towards more negative values. The mean values of $V_{1/2}$ were -68.12 ± 2.12

mV for control cells, -72.09 mV for OHP treated cells and -58.21 ± 072 mV for CDDP treated cells. *K* values were: 5.12 ± 0.98, 5.25 ± 0.26 and 7.79 ± 0.61 mV respectively. * p=0.005 for OHP *vs* CTRL (ANOVA, followed by the Tukey post hoc test).

Superimposing the activation and inactivation curves, the window current emerges from their intersection. This function describes the fraction of available channels at each Vm, at the steady-state: increasing the voltage makes the opening probability of the channels grow until the probability of inactivation prevails and so more and more channels inactivate until the complete abolition of the current.

From our experiments emerged that the treatment with OHP or CDDP for 24 h produced a window current whose amplitude and width was more than doubled compared to control conditions (**Figure 12**).

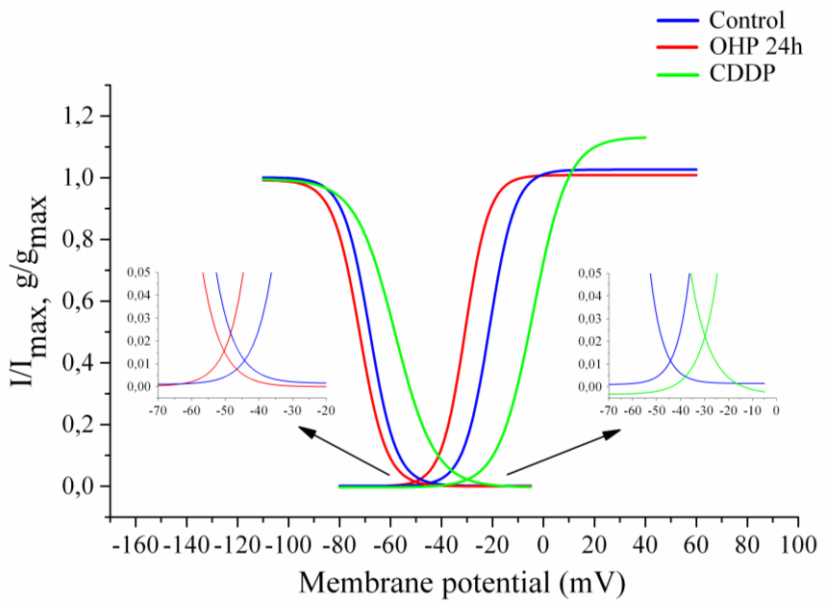

Figure 12. Effects of platinum analogues on the window current of voltage-dependent sodium channels. Representation of the window current through the superimposition of activation and inactivation curves. The curves built on data collected in non treated cells are represented in blue, the red ones describe the

voltage-dependence observed in cells treated with oxaliplatin (OHP) while the green ones represents the curves built on data collected in presence of cisplatin (CDDP).

Effects of platinum compounds on ERG potassium channel activation and inactivation curves

To study the voltage-dependence of ERG potassium channel activation we applied the stimulation protocol described in **figure 13A**. Also in this case, the experiments were performed using an external solution containing a high concentration of potassium (40 mM).

The curve was obtained by interpolating the values of the recorded peak currents (I, **Figure 13A** and **Figure 13B**) normalized on the amplitude of the maximal current observed (I_{max}) in relation to the applied membrane potential with a Boltzmann function:

$$\frac{I}{I_{max}} = \frac{1}{1 + e^{\frac{V_{1/2} - V_{pre}}{k}}}$$

where I_{max} is the maximum ERG current elicited after the most depolarized preconditioning potential, V_{pre} is the preconditioning potential, $V_{1/2}$ is the potential at which activation is half-maximal, and *k* is the slope factor.

The half-activation point ($V_{1/2}$) values were -32.22 ± 0.56 mV for the control and -26.08 ± 0.66 mV after the incubation for 24 h with OHP 7.5μM; the slope factor were 5 ± 0.43 mV and 5 ± 0.56 mV respectively. Thus, OHP produced a depolarizing shift of the activation curve of ERG currents (p=0.02). In contrast, CDDP administration did not produce any effect (**Figure 13C**).

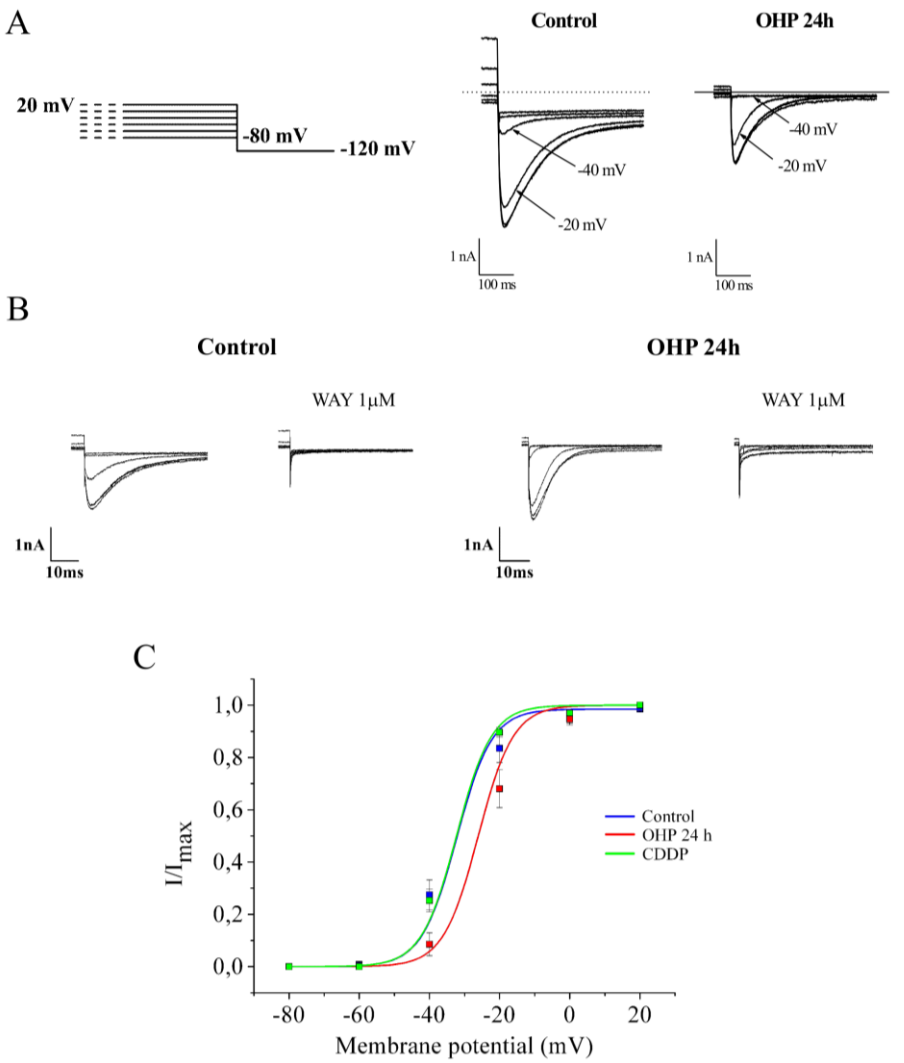

Figure 13. Voltage-dependence of ERG potassium channel activation in absence or presence of platinum drugs. **A.** Representative traces recorded using the protocol on the left in control conditions or in presence of oxaliplatin (OHP). **B.** Traces recorded in the presence or in the absence of WAY123.398 in control condition or after 24 h treatment with OHP. **C.** The blue curve represents data collected during control conditions (n=12), the red one shows the same property in cells after 24 h treatment with OHP (n=8) while the green one represent data collected in cells incubated with CDDP (n=6). The mean value of $V_{1/2}$ were -32.22 ± 0.56 mV for control cells, -26.08 ± 0.66 mV for cells treated with OHP and -33.72 ± 0.55 mV after the incubation with CDDP. The slope factor were 5 ± 0.43 mV, 5 ± 0.56 mV and 5.99 ± 0.39 mV respectively. $p<0.02$ for OHP *vs* CTRL (ANOVA, followed by the Tukey post hoc test).

To study the voltage-dependence of ERG channel inactivation we took advantage of a stimulation protocol during which, starting from a holding potential of 0 mV, applied voltage steps with duration of 184 ms and amplitude from +20 mV to -140 mV (decrement of 20 mV). At +20 mv, ERG channels are in the inactive state and no current flows through them (**Figure 14A**). However, in a few cells we observed a residual outward current due to the opening of outward potassium channels. In order to better isolate ERG current, the above protocol was performed in the presence of 1 µM WAY123.398 (Faravelli et al., 1996), a specific blocker of ERG channels at saturating concentration (**Figure 14B**). During data analysis, the traces recorded in these experimental conditions were subtracted to those collected in the absence of the blocker in order to isolate the WAY-sensitive ERG current. As the imposed membrane potential hyperpolarizes, inactivation is removed. At -140 mV the rapid voltage transition produces the complete opening of the channels, and the favorable driving force induces the maximal current.

From the recorded traces, ERG conductance was calculated with the equation:

$$g = \frac{I}{V_m - E_K}$$

Where I is the amplitude of the recorded current, V_m is the imposed membrane potential and E_K is the equilibrium potential for potassium ion. Data for each cell were fitted with a Boltzmann distribution equation of the following form:

$$\frac{g}{g_{max}} = \frac{1}{1 + e^{\frac{V_m - V_{1/2}}{k}}}$$

where g_{max} is the maximum g, $V_{1/2}$ is the potential at which channel activation is half-maximal, and k is the slope of the curve.

Figure 14C shows that the incubation with OHP for 24 h determined a shift of the inactivation curve of ERG channels towards more hyperpolarized membrane potentials ($p<0.001$). The estimated average values for $V_{1/2}$ were -56.46 ± 3.09 mV in control cells and -78.50 ± 2.88 mV in treated cells, with a slope factor (k) of 12 or both curves.

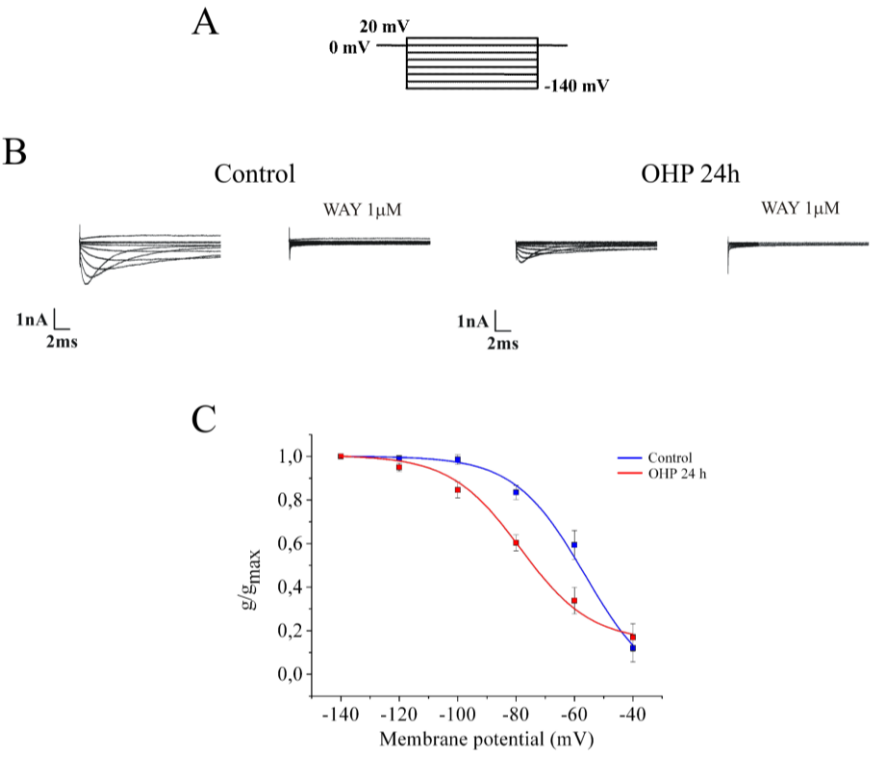

Figure 14. Voltage-dependence of ERG potassium channel inactivation under control conditions and in the presence of oxaliplatin (OHP). A. Graphical representation of the protocol in voltage-clamp mode used for the investigation of the voltage-dependence of ERG channel inactivation**. B.** Traces recorded in the

presence or in the absence of WAY123.398 in control condition or after 24 h treatment with OHP. **C.** OHP incubation caused a shift of the inactivation curve of ERG channels to more negative membrane potentials. The blue curve represents data collected during control conditions (n=7) while the red curve shows data collected in OHP treated cells (n=10). The average values of $V_{1/2}$ were -56.46 ± 3.09 mV in control cells and -78.50 ± 2.88 mV in treated cells, with a slope factor of 12 for both curves. P<0.001 (ANOVA, followed by the Tukey post hoc test).

Figure 15 shows the activation and inactivation curves in the absence (blue) and in presence of OHP treatment (red). As a consequence of the properties of ERG channel inactivation kinetics it was not possible to measure ERG current window.

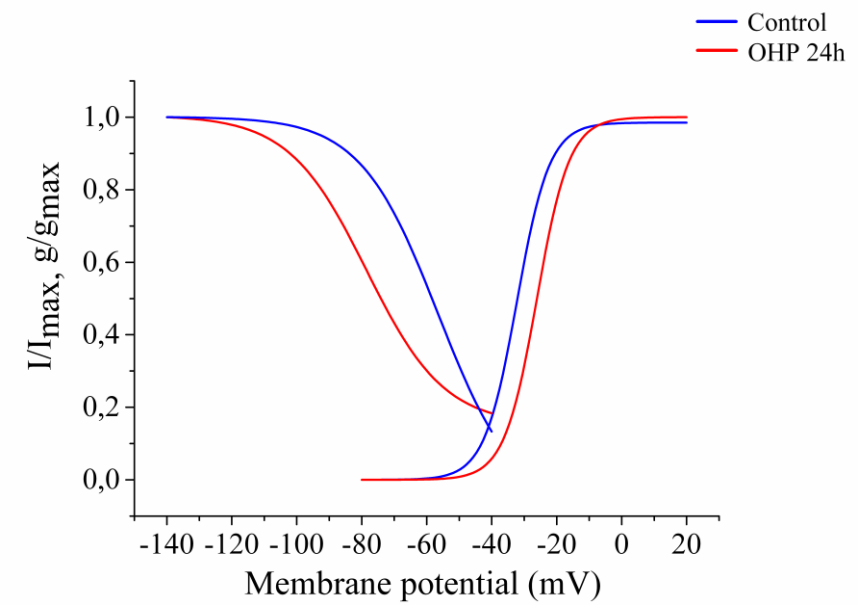

Figure 15. Effect of oxaliplatin (OHP) on the window current of ERG channels. Representation of the window current through the superimposition of activation and inactivation curves. The curves built on data collected in non treated cells are represented in blue while the red ones describe the properties observed in cells treated with OHP for 24 h.

3.2 Effects of OHP on primary cultures of embryonic rat DRG sensory neurons

Since F-11 cells are somatic cell hybrid of rat embryonic DRGs and mouse neuroblastoma cell line N18TG-2, the experiments formerly described were reproduced on primary cultures of sensory neurons deriving from the dissociation of rat embryonic DRGs. This choice was motivated by the necessity to validate differentiated F-11 cell line as a model of sensory neurons for studying platinum-derivate effects.

3.2.1 Effect of OHP on the electrical activity

Influence of OHP treatment on V_{Rest}

Embryonic sensory neurons were analyzed by patch-clamp after 36 and 48 h of incubation with 7.5 μM OHP incubation. **Figure 16** shows that both treatments determined a non-significant effect on V_{Rest}.

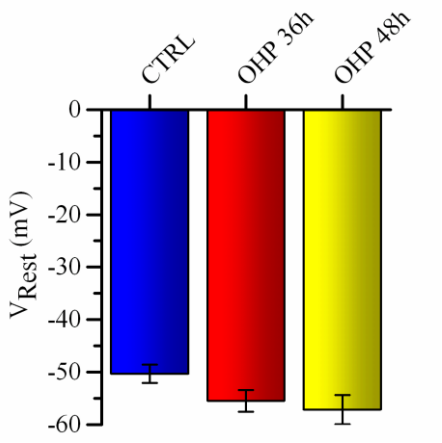

Figure 16. Effects of different oxaliplatin (OHP) incubation on membrane potential (V_{Rest}). OHP determined a progressive but non-significant hyperpolarization of V_{Rest}. The observed mean values were: -50.31 ± 1.73 mV in non-treated cells (n=16), -55.47 ± 2.07 mV in cells treated with OHP for 36 h (n=17) and -57.16 ± 2.77 mV in cells incubated with OHP for 48 h (n=12) (ANOVA, followed by the Tukey post hoc test).

Effect of OHP on induced APs

Evoked APs were studied through the application of the stimulation protocol previously described (**Figure 3A**). In each tested cell, firing frequencies were calculated referring to the injected current step during which the maximal number of evoked APs was observed (**Figure 17**).

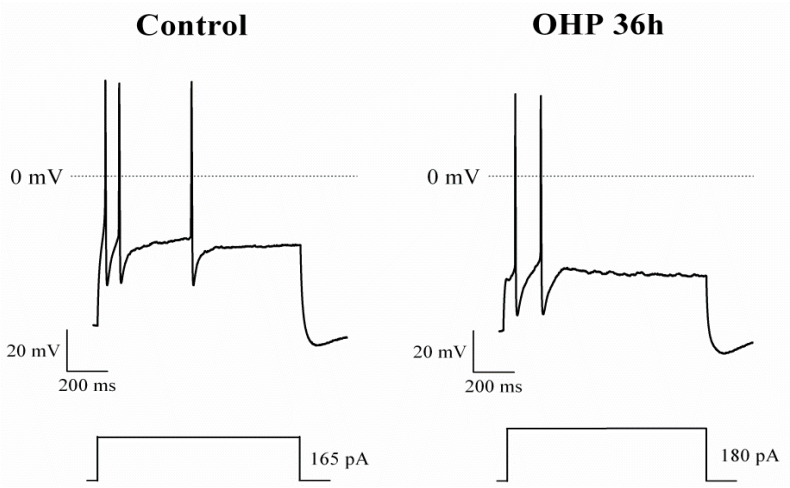

Figure 17. Representative traces of the evoked electrical activity of embryonic DRG neurons recorded in control conditions or after 36 h treatment with OHP using the protocol described below the traces.

Incubation with OHP for 36 h did not produce any major variation of the AP firing frequency. After 48 h, treated cells showed a non-significant increase of the same feature (**Figure 18**). However, statistical analysis with χ^2 test revealed for 48 h OHP a significant increase of the fraction of sensory neurons able to fire multiple evoked APs compared to the non-treated control cells ($p < 0.033$).

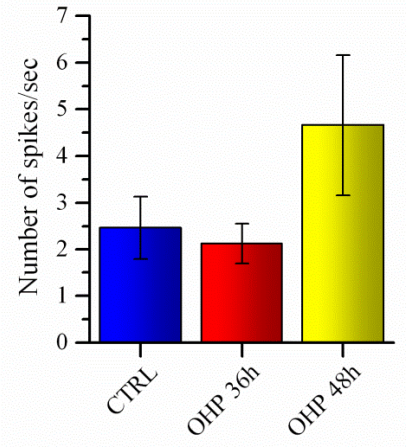

Figure 18. Effects of the incubation with oxaliplatin (OHP) on evoked firing frequency. The histogram shows that the administration of OHP for 48 h seemed to produce an increase of evoked APs firing frequency, which was not significant. The observed average values were: 2.46 ± 0.67 Hz in control cells (n=13), 2.12 ± 0.43 Hz in cells treated with OHP for 36 h (n=16) and 4.66 ± 1.50 Hz in cells incubated with OHP for 48 h (n=12) (ANOVA, followed by the Tukey post hoc test).

3.2.2 OHP administration affected voltage-dependent sodium and delayed rectifier potassium currents

The effects of OHP on voltage-dependent sodium and potassium channels were studied by applying the formerly described stimulation protocol (**Figure 5A**). Collected data showed that treating the cells with OHP produced a progressive increase of the current density of the voltage-dependent sodium channels. (**Figure 19 A-B**).

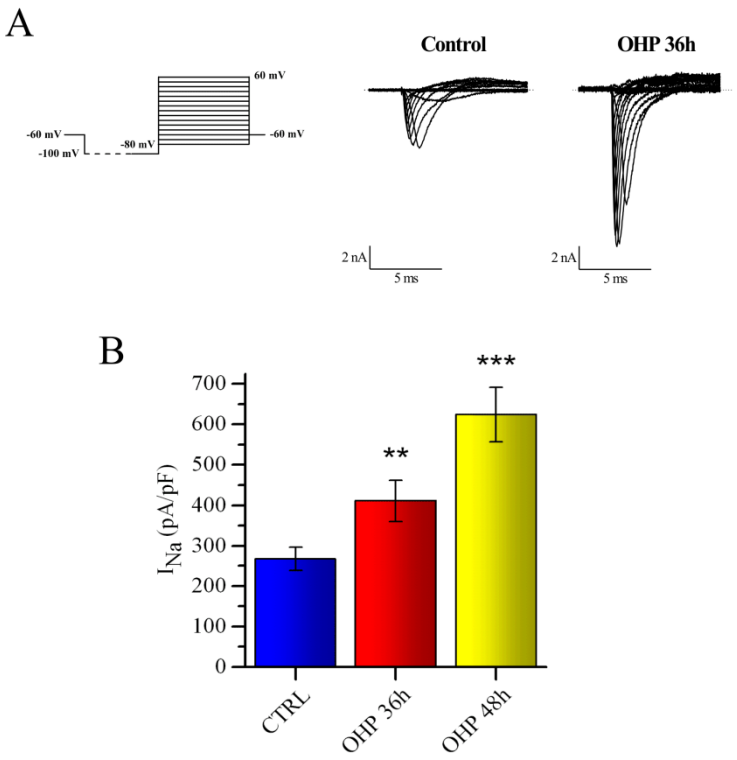

Figure 19. Effects of oxaliplatin (OHP) on voltage-dependent sodium channels. **A.** Representative current traces recorded in absence or in presence of OHP for 36h. **B.** OHP determined an increase of sodium current densities in treated cells compared to controls. The observed mean values were: 267.14 ± 29.21 pA/pF in control cells (n=17), 411 ± 50.68 pA/pF in cells treated with OHP for 36 h (n=15) and 623.74 ± 67.23 pA/pF in cells incubated with OHP for 48 h (n=12). **p<0.01 for OHP 36 h *vs* CTRL, ***p<0.001 for OHP 48 h *vs* CTRL (ANOVA, followed by the Tukey post hoc test).

Since DRG neurons also express TTX-resistant sodium currents, we investigated the possible effects of OHP on these currents. The incubation with OHP did not induce any change of TTX-resistant sodium current densities and of their fraction respect to the total sodium current (**Figure 20**). The mean observed values (in percentage) were: 15.16 ± 7.06 % in control cells (n=10), 13.56 ± 8.05

% in OHP 36 h treated cells (n=10) and 6.37 ± 3.25 % in 48 h treated cells (n=8).

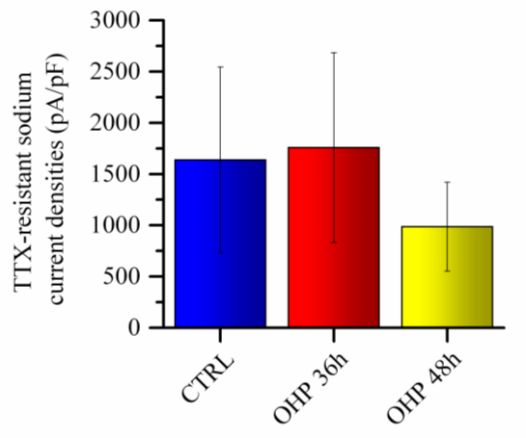

Figure 20. Effects of different oxaliplatin (OHP) incubation on the TTX-resistant sodium current densities. The histogram shows that the exposure to OHP for 36 or 48 h did not produced any effect on TTX-resistant sodium current densities compared to control conditions. The mean values observed were: 1638 ± 906 pA/pF for control cells (n=8), 1759 ± 927 pA/pF for cells treated with 36 h OHP (n=5) and 986 ± 433 pA/pF for OHP treated cells for 48 h (n=4) (ANOVA, followed by the Tukey post hoc test).

The sodium current inactivation kinetics were analyzed considering the trace of the first current elicited by the stimulation protocol described in **figure 11**. This trace was obtained by a voltage step at 0 mV. The kinetic was described by the tau (τ, expressed in µs) parameter that was determined from single exponential fits of the current decay. The function used during the fitting procedure was:

$$f(t) = Ae^{-t/\tau} + C$$

Where A is the amplitude of the repolarization, τ is the time constant and C is the constant y-offset.

Figure 21 shows that the incubation with OHP for 36 or 48 h did not affect this parameter.

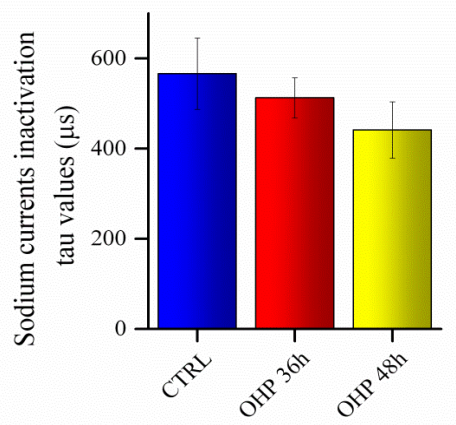

Figure 21. Effects of different oxaliplatin (OHP) incubation on voltage-dependent sodium channel inactivation kinetics. OHP treatment did not induce any effect on the time constant describing the decay of the recorded currents. The mean values observed were: 566 ± 79 µs in control cells (n=8), 512 ± 45 µs in 36 h OHP treated cells (n=5) and 441 ± 62 µs in cell incubated with OHP for 48 h (n=4) (ANOVA, followed by the Tukey post hoc test).

We then focused on the current densities of delayed-rectifier potassium channels. In this regard, our data showed that incubating the cells with OHP determined a significant increase of current densities (**Figure 22**).

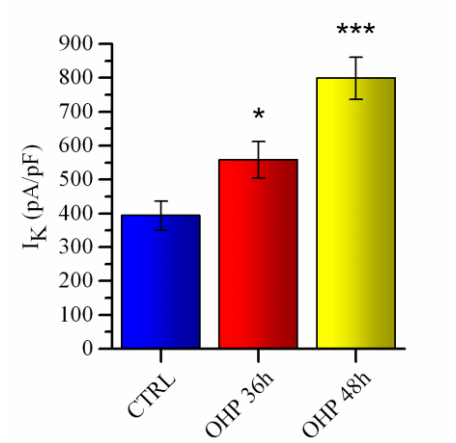

Figure 22. Effects of oxaliplatin (OHP) on delayed-rectifier potassium current densities. OHP determined an increase in treated cells compared to controls. The mean observed values were: 393.50 ± 43.38 pA/pF in non treated cells (n=17), 558.58 ± 54.19 pA/pF in cells treated for 36 h (n=15) and 799.08 ± 62.19 pA/pF in cells incubated with OHP for 48 h (n=12). *$p<0.05$ for OHP 36h vs CTRL, ***$p<0.001$ for OHP 48 h vs CTRL (ANOVA, followed by the Tukey post hoc test).

3.3 Effects of OHP on primary cultures of adult rat DRG sensory neurons

Finally, the effects of 7.5 µM OHP on cell electrical properties and on voltage-dependent sodium and potassium channels were tested in primary cultured sensory neurons derived from adult rat DRGs, after 7 days in vitro (DIV).

3.3.1 OHP administration did not alter the overall electrical activity

Incubation with OHP for 24 h did not produce any significant variation of V_{Rest} (**Figure 23**).

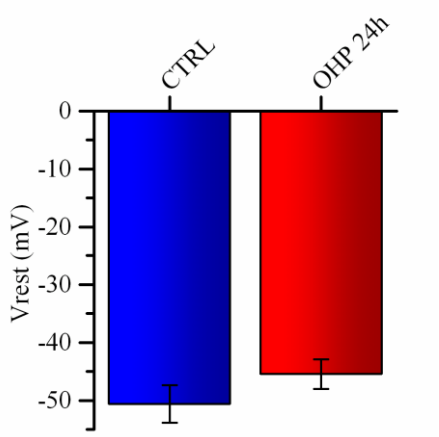

Figure 23. Influence of oxaliplatin (OHP) on membrane resting potential (V_{Rest}). The 24 h-long treatment with OHP did not affect the V_{Rest} of the tested cells. The mean values were: -50.62 ± 3.24 mV in control cells (n=8) and -45.44 ± 2.57 mV in cells treated with OHP (n=9) (Student's *t*-test).

Also in this case, evoked APs were studied by means of the application of the stimulation protocol described below the traces and the firing frequencies were calculated referring to the injected current step during which the maximal number of APs was evoked. **Figure 24**

A-B shows that, after the treatment with OHP, we did not detect any significant variation of this parameter.

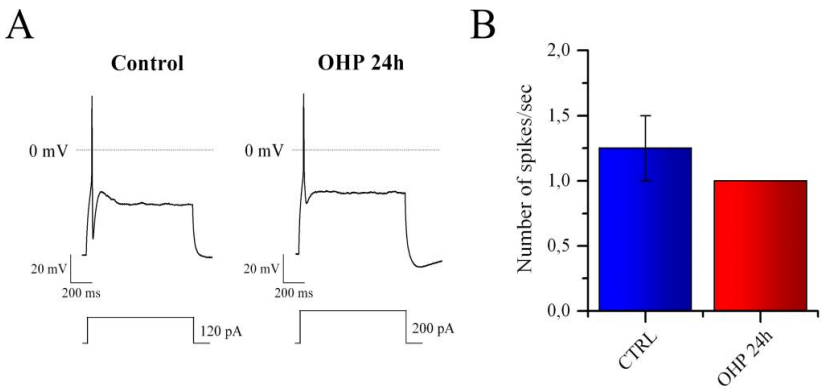

Figure 24. Effects of oxaliplatin (OHP) on AP firing frequency. A. Representative traces of the evoked electrical activity of adult DRG neurons recorded in control conditions or during OHP treatment, using the protocol below the traces. **B.** OHP did not alter the AP firing frequency in tested cells. The mean observed values were: 1.25 ± 0.25 Hz in non treated cells (n=4) and 1 Hz in the cells incubated with OHP for 24 h (n=9). All OHP treated cells showed only one AP during the stimulation protocol (Student's *t*-test).

3.3.2 Effects of OHP on voltage-dependent sodium and potassium channels

In order to evaluate possible alterations produced by OHP on voltage-dependent sodium and potassium channels, we used the stimulation protocol described in **figure 5A**.

Data showed that the incubation with OHP for 24 h increased the current density of voltage-dependent sodium channels. The mean values were: 139.63 ± 27.26 pA/pF in control cells (n=8) and 359.17 ± 46.10 pA/pF in treated cells (n=9) (**Figure 25**).

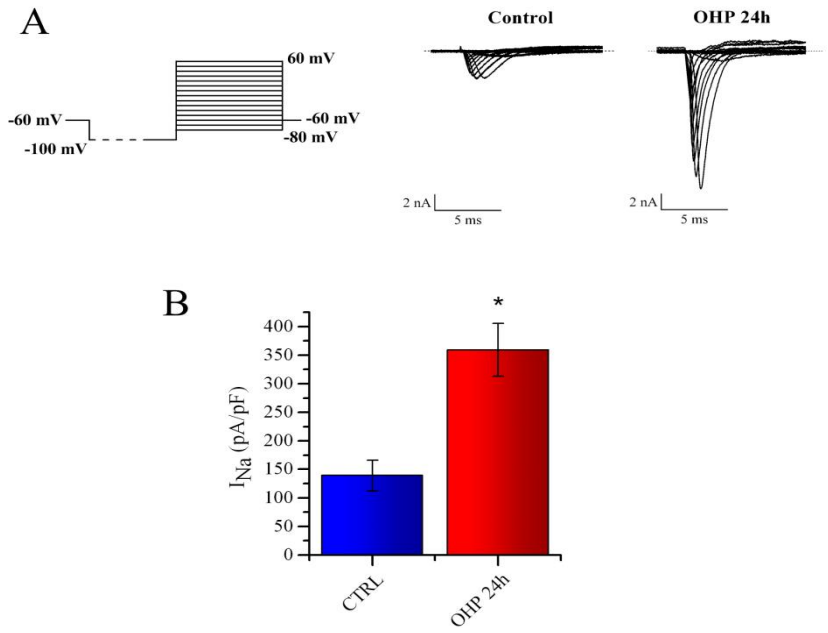

Figure 25. Effects oxaliplatin (OHP) on voltage-dependent sodium channels. **A.** Representative traces recorded in absence or in presence of OHP for 24 h. **B.** OHP application determined a significant increase of the sodium current density compared to control cells. The average observed values were: 139.63 ± 27.26 pA/pF in control cells (n=8) and 359.17 ± 46.10 pA/pF in treated cells (n=9). *p<0.05 for OHP 24 h *vs* CTRL (Student's *t*-test).

Moreover, incubation with OHP did not induce any change in the TTX-resistant sodium current densities and in their fraction referred to the total sodium current (**Figure 26**). The mean values (in percentage) were: 33 ± 14.33 % in control cells (n=4), 5 ± 1 % in cells treated with OHP for 24 h (n=7).

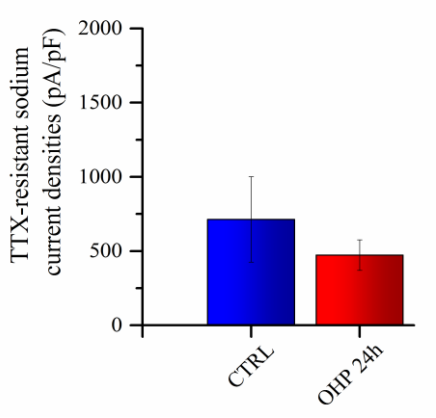

Figure 26. Effects of oxaliplatin (OHP) incubation on the TTX-resistant sodium current densities. OHP exposure for 24 h did not produce any effect on TTX-resistant sodium current densities compared to control conditions. The mean values were: 713 ± 287 pA/pF for control non-treated cells (n=3), 473 ± 103 pA/pF for cells treated with OHP 24 h (n=6) (Student's *t*-test).

The sodium current inactivation kinetics were analyzed as previously described for embryonic DRG neurons. **Figure 27** shows that OHP treatment did not produce any effect on τ values.

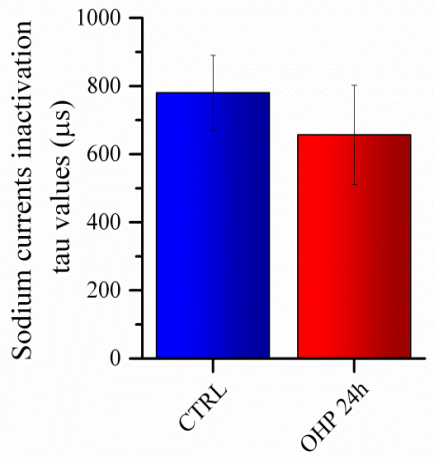

Figure 27. Effects of different oxaliplatin (OHP) incubation on voltage-dependent sodium channels inactivation kinetics. OHP treatment did not induce any effect on the time constant describing the decay of the recorded currents. The

mean values observed were: 780 ± 110 μs in control cells (n=2), 656.7 ± 145.8 μs in OHP treated cells (n=6) (Student's *t*-test).

An increasing trend was also observed on the current density of voltage-dependent potassium channels but, in this case, the effect did not reach the statistical significance. The mean values of current density were: 238 ± 39 pA/pF in control cells (n=8) and 302 ± 37 pA/pF in cells treated with OHP for 24 h (n=9) (**Figure 28**).

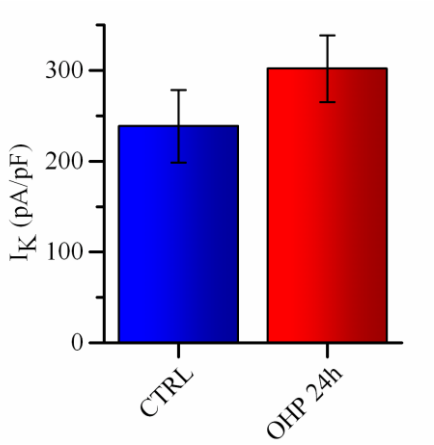

Figure 28. Effects of oxaliplatin (OHP) on delayed-rectifier potassium current densities. In treated cells, OHP produced a non-significant increase of the current density of voltage dependent potassium channels compared to controls. The mean values of current density were: 238 ± 39 pA/pF in control cells (n=8) and 302 ± 37 pA/pF in cells treated with OHP for 24 h (n=9) (Student's *t*-test).

3.4 Result summary

All the obtained results are summarized in **Table 5.**

***In vitro* model used**	**[platinum] and timing**	**Effects on cellular electrical activity**	**Effects on ion channels**
F-11 differentiated cells	OHP 7.5 µM 24h	Depolarized V_{Rest} Depolarized AP afterhyperpolarization.	↑ Na^+ current density, ↓ ERG current density, shift of Na^+ activation curve towards more negative values, shift of Na^+ inactivation curve towards more negative values, shift of ERG activation curve towards more negative values, shift of ERG inactivation curve towards more negative values
	OHP 7.5 µM 48h	Depolarized V_{Rest} ↓ spontaneous electrical activity ↓ evoked firing frequency Depolarized AP afterhyperpolarization.	↑ Na^+ current densities
	CDDP 15 µM	↓ evoked firing frequency ↑ AP amplitude ↑ AP duration Depolarized AP afterhyperpolarization.	↓ Na^+ current density ↓ K^+ delayed rectifier current density ↓ ERG current density Shift of Na^+ activation curve towards more positive values Shift of Na^+ inactivation curve towards more positive values
Embryonic rat DRG sensory neurons	OHP 7.5 µM 36h	-	↑ Na^+ current density ↑ K^+ delayed rectifier current density
	OHP 7.5 µM 48h	↑ fraction of sensory neurons able to fire multiple evoked APs	↑ Na^+ current density ↑ K^+ delayed rectifier current density
Adult rat DRG sensory neurons	OHP 7.5 µM 24h	-	↑ Na^+ current density

Table 5. Result summary. Summary of the effects observed after OHP or CDDP treatment described in this chapter.

4. DISCUSSION AND FUTURE PERSPECTIVES

OHP is a third generation platinum-based compound used in combination with folinic acid (Leucovorin) and 5-fluorouracil (FOLFOX regimen), for first-line and adjuvant metastatic colorectal cancer therapy (Chau and Cunningham, 2003). OIPN represents one of the most common adverse events associated with the use of OHP, which can reduce patients' quality of life and lead to dose reduction or discontinuation of the treatment. OIPN has unique characteristics, in fact, it is associated with two different syndromes: an acute and cold-induced transient syndrome occurring in almost all patients and a dose-limiting chronic sensory neuropathy (Grothey, 2003). It has been demonstrated that the incidence and severity of acute OIPN is predictive for the development of the chronic and cumulative sensory neuropathy (Argyriou et al., 2013a; Valesco et al., 2014). For this reason, understanding acute OIPN pathogenesis is essential in order to develop preventive strategies for chronic OIPN.

Acute OIPN is described in literature as a channelopathy-like syndrome, in fact, needle electromyography examinations and motor nerve conduction studies reveal spontaneous high frequency discharges of motor fibres and repetitive compound motor action potentials (CMAPs) in response to a single electrical stimulus in the following 24-48 h after OHP infusion (Wilson et al., 2002; Lehky et al., 2004). Moreover, the results from nerve excitability testing demonstrate an increase of refractoriness in motor axons and a decrease of the same parameter in sensory axons (Krishnan et al., 2005, 2006; Park et al., 2009). These findings, together with the results of recent pharmacogenomics studies that have identified

polymorphisms in genes encoding for voltage-dependent sodium channels (Argyriou et al., 2013b) related to the onset of acute OIPN, support the hypothesis of a major involvement of sodium channels in acute OIPN pathogenesis.

Since early 2000, many *in vitro* studies have investigated the effects of this platinum based antineoplastic agent on voltage-dependent sodium and potassium channels, the main effectors of electrical neuronal activity. These researches focused on single aspects of the overall electrophysiological cellular response to OHP and were conducted on different preparations and cellular models using OHP applied extracellularly or intracellularly in concentrations ranging from 5 to 500 μM. These concentrations are sometimes very far from the peak values observed in the blood of treated patients (i.e. 1.44 μg/ml, corresponding to 3.6 μM, after 2h infusion for a dose of 85 mg/m^2 and 2.59-3.22 μg/ml, corresponding to 6.8 – 8.11 μM, after 2h infusion for a dose of 130 mg/m^2, Ehrsson et al., 2002; Graham et al., 2000). As a result, different effects have been reported involving sodium, potassium and calcium channels sometimes with discordant outcomes. For this reason, we decided to investigate the acute effects of an OHP concentration comparable to the one estimated in patients' blood (7.5 μM for 24 or 48 h) on the cellular electrical properties of differentiated F-11 cells. These are hybrids of rat embryonic dorsal root ganglia (DRG) and mouse neuroblastoma cell line N18TG-2, which represent a good cellular model of DRG neurons. Subsequently, the same set of experiments was performed on neuron primary cultures deriving from embryonic and adult DRG dissociation. Moreover, since clinical data show that CDDP administration does not

produce the acute symptoms of peripheral neurotoxicity described for the patients treated with OHP (Lehky et al., 2004), we used CDDP as reference compound to verify the exclusivity of the effects induced by OHP, as previously proposed by Grolleau and colleagues (2001).

Data collected on differentiated F-11 cells indicate that, compared to controls, cells treated with OHP showed significantly depolarized V_{Rest} and after-hyperpolarization potentials that are consistent with the hyperexcitability effect reported in literature. In fact, cells showing a more depolarized V_{Rest} and a smaller after-hyperpolarization are more prone to generate APs in response to a stimulation and to give rise to bursts of APs. On the contrary, incubation with CDDP did not produce any alteration of V_{Rest}. However, both OHP and CDDP treatment induced a significant decrease in firing frequencies. Moreover, the incubation with OHP determined a reduction in the percentage of cells showing spontaneous electrical activity compared to control and CDDP treated cells.

To understand which mechanisms were responsible for these changes in the cellular electrical activity we studied the effects of platinum compounds on voltage-dependent ion channels. As previously described by Adelsberger et al. (2000), prolonged OHP incubation caused an increase in sodium current density.

Since differentiated F-11 cells express ERG (*ether-à-go-go related* gene) channels, we also investigated the possible effects of OHP on these channels. ERG is a voltage-dependent potassium channel, acting as a functional inward rectifier. It was first identified in a *Drosophila melanogaster* mutant and only years later an homolog was found in

humans, during a screening of an hippocampal cDNA library, and mapped to chromosome 7 (Warmke et Ganetzky, 1994). ERG channels are very important in the heart where they play a key role in the AP repolarization. Mutations in hERG genes are related to an hereditary disorder, the long QT syndrome (Curran et al., 1995). Moreover, ERG channels are involved in the release of insulin by human pancreatic β cells (Rosati et al., 2000), and members of its family are expressed in tumors of different histogenesis, where they regulate the neoplastic progression (Arcangeli et al., 2009). In the central nervous system (CNS) the ERG function is still debated (Shi et al.,1997; Saganich et al., 2001; Guasti et al., 2005; Bauer and Schwarz, 2018). The ERG potassium channel family is composed by three different isoforms. To date, there are no clues in literature about which isoforms are effectively expressed in F-11 cells. However, considering that this cell line is a hybrid of rat DRG neurons and a neuroblastoma cell line, we hypothesize that all the three isoforms of ERG channels (Shi et al., 1997) are expressed as suggested by the value of the $V_{1/2}$ of the activation curves we obtained. Unfortunately, since there are no available blockers specific for the different ERG channel isoforms, we were not able to isolate the single currents and perform further investigations.

Our data showed that OHP incubation decreased ERG potassium current density. In differentiated F-11 cells no effects on other potassium channels were observed.

In the same experimental conditions, CDDP treatment decreased both voltage-dependent sodium and potassium current densities.

Based on these data, to better characterize the effects of these platinum-based antineoplastic agents on sodium and ERG potassium channels, F-11 cells were incubated with these compounds for 24h and the biophysical properties of activation and inactivation were investigated. According to previously reported results, the analysis of TTX-sensitive sodium currents indicated that OHP treatment induced a shift of both activation and inactivation curves towards more negative potentials and an increase in the current window (> 2.5 fold) (Adelsberger et al., 2000; Benoit et al., 2001). In contrast, cells treated with CDDP showed an opposite behavior represented by a shift of both activation and inactivation curves towards more positive potentials and a smaller increase in the current window.

The analysis of the biophysical properties of ERG potassium channels showed that OHP treatment induced a shift of the activation curve towards more positive potentials and of the inactivation curve towards more negative potentials. The incubation with CDDP had no effect on ERG channel activation.

These effects on both sodium and ERG potassium channels may explain the membrane depolarization and the change in the firing rate we recorded in OHP treated cells. In particular, the reduced firing rate could be more likely linked to the shift of the window current towards more negative membrane potentials rather than to the effect we observed on ERG channels. In fact, it has been described that the reduction of ERG channel activity by a selective inhibitor induced an increase in the firing frequency (Chiesa et al., 1997; Rosati et al., 2000). However, as reported in literature, a compensatory increase of other potassium currents cannot be excluded (Pillozzi et al., 2018).

These results were partially confirmed in the set of experiments conducted on embryonic or adult rat DRG neuronal primary cultures. In fact, our data showed that OHP treatment had no effects on V_{Rest} and on the firing frequency even if an increase in the percentage of neurons able to generate multiple evoked APs was observed. The analysis of sodium and potassium current densities revealed their increase. Conversely from the article of Loligner et al. (2015) that linked cold-induced allodynia to the effects of OHP on sodium channel $Na_v1.9$, we did not observed any alteration in TTX-resistant sodium current densities in treated cells compared to controls. Moreover, in these models we were not able to evaluate the effects of OHP on ERG potassium channels because no currents were recorded during the experiments. This suggests that ERG channels are not expressed in DRG neurons.

Our work gives a general overview on the OHP effects on the electrical properties of the tested cells, evaluating not only its influence on the V_{Rest} and APs but also on the voltage-dependent sodium and potassium channel properties. Moreover, all the experiments were conducted using an OHP concentration that best represents the one reached in the plasma of patients after the drug infusion. The increase in the number of cells able to fire multiple spontaneous APs we observed in the experiments conducted on DRG primary cultures seems to be in line with the hyperexcitability phenomena reported in patients in the following 24-48 h after OHP infusion. On the other hand, data collected on differentiated F-11 cells seem to reproduce an intermediate condition between the acute and

the chronic OHP toxicity in which an initial phase of hyperexcitability is followed by a state of hypoexcitability.

In conclusion, data collected on DRG primary neurons indicate that differentiated F-11 cells may represent a good cellular model for the study of the effects of platinum-based compounds on voltage-dependent sodium channels. In fact, the effects we recorded on voltage-dependent potassium channels might be discordant owing to the different channel subtypes expressed by differentiated F-11 cells and DRG neurons.

Future perspectives

Further developments of this study will encompass three main experimental strategies on different biological substrates in order to maximize the translational impact.

We will first evaluate the effects of CDDP on embryonic or adult rat DRG neuron primary cultures. In this way, we will be able to compare the influence of these platinum compounds on the cellular electrical activity also in these *in vitro* models. Since DRG neurons are the main target of platinum analogues and CDDP administration is not linked to the development of acute toxicity, this approach may represent a key step in the understanding of the mechanisms underlying acute OIPN.

We will then study the effects of platinum compounds on neurons derived from induced pluripotent stem cells (IPSC). As this technology allows the culturing of human derived sensory neurons overcoming the problem of sample harvesting, they may represent the ideal *in vitro* model to investigate the patophysiology of OIPN.

Thus, in case of promising results, we will study the effects of pharmacological strategies in order to find potential drugs with protective/reverting activity. For this purpose, we will focus on the study of the effects of Ca/Mg administration and on voltage-dependent sodium channel modulators. In fact, literature data indicate that supplemental Ca/Mg infusions may reduce OHP neurotoxicity but more investigations are needed to fully confirm the efficacy of this pharmacological approach (De Monaco et al., 2014). Based on the results of this *in vitro* screening we will test the effects of promising drugs in an *in vivo* model of OIPN.

Lastly, further studies could be focused on the evaluation of the effects of OHP on differentiated DRG neurons derived from IPSC of patients carrying sodium channels polymorphisms known to be associated to a major incidence and severity of OIPN.

5. BIBLIOGRAPHY

Addington J, Freimer M. Chemotherapy-induced peripheral neuropathy: an update on the current understanding' *F1000Research*. 2016;5.

Adelsberger H, Quasthoff S, Grosskreutz J, Lepier A, Eckel F, Lersch C. The chemotherapeutic oxaliplatin alters voltage-gated Na^+ channel kinetics on rat sensory neurons. *European Journal of Pharmacology*. 2000;406(1):25-32.

Alberti P, Rossi E, Cornblath DR, Merkies I.S, Postma TJ, Frigeni B, Bruna J, Velasco R, Argyriou AA, Kalofonos HP, Psimaras D, Ricard D, Pace A, Galiè E, Briani C, Dalla Torre C, Faber CG, Lalisang RI, Boogerd W, Brandsma D, Koeppen S, Hense J, Storey D, Kerrigan S, Schenone A, Fabbri S, Valsecchi MG, Cavaletti G; CI-PeriNomS Group. Physician-assessed and patient-reported outcome measures in chemotherapy-induced sensory peripheral neurotoxicity: two sides of the same coin. *Annals of oncology*. 2014;25(1):257-64.

Albers JW, Chaudhry V, Cavaletti G, Donehower RC. Interventions for preventing neuropathy caused by cisplatin and related compounds. *The cochrane database of systematic reviews*. 2014;(3):CD005228.

Alcindor T, Beauger N. Oxaliplatin: a review in the era of molecularly targeted therapy. *Current oncology*. 2011 Jan;18(1):18-25.

Ali I, Wani WA, Saleem K, Haque A. Platinum compounds: a hope for future cancer chemotherapy. *Anticancer agents in medicinal chemistry*. 2013;13(2):296-306.

Allodi I, Udina E, Navarro X. Specificity of peripheral nerve regeneration: interactions at the axon level. *Progress in neurobiology*. 2012;98(1):16-37.

Arcangeli A, Crociani O, Lastraioli E, Masi A, Pillozzi S, Becchetti A. Targeting ion channels in cancer: a novel frontier in antineoplastic therapy. *Current medicinal chemistry*. 2009;16(1):66-93.

Argyriou AA, Polychronopoulos P, Iconomou G, Chroni E, Kalofonos HP. A review on oxaliplatin-induced peripheral nerve damage. *Cancer treatment reviews*. 2008;34(4):368-77.

Argyriou AA, Bruna J, Marmiroli P, Cavaletti G. Chemotherapy-induced peripheral neurotoxicity (CIPN): an update. Critical reviews in oncology/hematology. 2012;82(1):51-77.

Argyriou AA, Cavaletti G, Briani C, Velasco R, Bruna J, Campagnolo M, Alberti P, Bergamo F, Cortinovis D, Cazzaniga M, Santos C, Papadimitriou K, Kalofonos HP. Clinical pattern and associations of oxaliplatin acute neurotoxicity: a prospective study in 170 patients with colorectal cancer. *Cancer*. 2013a;119(2):438–44.

Argyriou AA, Cavaletti G, Antonacopoulou A, Genazzani AA, Briani C, Bruna J, Terrazzino S, Velasco R, Alberti P, Campagnolo M, Lonardi S, Cortinovis D, Cazzaniga M, Santos C, Psaromyalou A, Angelopoulou A, Kalofonos HP. Voltage-gated sodium channel polymorphisms play a pivotal role in the development of oxaliplatin-induced peripheral neurotoxicity: results from a prospective multicenter study. *Cancer*. 2013b;119(19):3570-7.

Argyriou AA, Kyritsis AP, Makatsoris T, Kalofonos HP. Chemotherapy-induced peripheral neuropathy in adults: a comprehensive update of the literature. *Cancer management research.* 2014; 6:135-47.

Argyriou AA, Bruna J, Genazzani AA, Cavaletti G. Chemotherapy-induced peripheral neurotoxicity: management informed by pharmacogenetics. *Nature Reviews Neurology*. 2017;13(8):492-504.

Avan A, Postma TJ, Ceresa C, Avan A, Cavaletti G, Giovannetti E, Peters GJ. Platinum-induced neurotoxicity and preventive strategies: past, present, and future. *Oncologist*. 2015;20(4):411-32.

Bakogeorgos M, Georgoulias V. Risk-reduction and treatment of chemotherapy-induced peripheral neuropathy. *Expert review of anticancer therapy*. 2017;17(11):1045-1060.

Banach M, Juranek JK, Zygulska AL. Chemotherapy-induced neuropathies-a growing problem for patients and health care providers. *Brain and Behavior*. 2017;7(1):e00558.

Bauer CK, Schwarz JR. Ether-à-go-go K(+) channels: effective modulators of neuronal excitability. *The journal of physiology*. 2018;596(5):769-783.

Benoit E, Brienza S, Dubois JM. Oxaliplatin, an anticancer agent that affects both Na+ and K+ channels in frog peripheral myelinated axons. *General Physiology Biophysics*. 2006;25(3):263-76.

Biedler JL, Roffler-Tarlov S, Schachner M, Freedman LS. Multiple neurotransmitter synthesis by human neuroblastoma cell lines and clones. *Cancer research.* 1978;38(11 Pt 1):3751-7.

Brewer JR, Morrison G, Dolan ME, Fleming GF. Chemotherapy-induced peripheral neuropathy: current status and progress. *Gynecologic oncology*. 2016;140(1):176-183.

Broomand A, Jerremalm E, Yachnin J, Ehrsson H, Elinder F. Oxaliplatin neurotoxicity--no general ion channel surface-charge effect. *Journal of negative results in biomedicine*. 2009;8:2.

Brouwers EE, Huitema AD, Boogerd W, Beijnen JH, Schellens JH. Persistent neuropathy after treatment with cisplatin and oxaliplatin. Acta Oncologica. 2009;48(6):832-41.

Burger H, Zoumaro-Djayoon A, Boersma AW, et al. Differential transport of platinum compounds by the human organic cation transporter hOCT2 (hSLC22A2). *Br J Pharmacol*. 2010;159(4):898-908.

Canetta R, Rozencweig M, Carter S.K. Carboplatin: the clinical spectrum to date. *Cancer treatment reviews*. 1985;12 suppl A:125-36.

Canta A, Pozzi E, Carozzi VA. Mitochondrial Dysfunction in Chemotherapy-Induced Peripheral Neuropathy (CIPN). Bellinger D, ed. *Toxics*. 2015;3(2):198-223.

Carozzi VA, Canta A, Chiorazzi A. Chemotherapy-induced peripheral neuropathy: What do we know about mechanisms? *Neuroscience Letters*. 2015;596:90-107.

Cassidy J, Misset JL. Oxaliplatin-related side effects: characteristics and management. *Seminars in oncology*. 2002;29(5 Suppl 15):11-20.

Cassidy J, Tabernero J, Twelves C, Brunet R, Butts C, Conroy T, Debraud F, Figer A, Grossmann J, Sawada N, Schöffski P, Sobrero A, Van Cutsem E, Díaz-Rubio E. XELOX (capecitabine plus oxaliplatin): active first-line therapy for patients with metastatic colorectal cancer. Journal of clinical oncology. 2004;22(11):2084-91.

Cata JP, Weng HR, Burton AW, Villareal H, Giralt S, Dougherty PM. Quantitative sensory findings in patients with bortezomib-induced pain. *Journal of pain*. 2007;8:296–306.

Cavaletti G, Zanna C. Current status and future prospects for the treatment of chemotherapy-induced peripheral neurotoxicity. *European journal of cancer*. 2002;38(14):1832-7.

Cavaletti G, Frigeni B, Lanzani F, Mattavelli L, Susani E, Alberti P, Cortinovis D, Bidoli P. Chemotherapy-Induced Peripheral Neurotoxicity assessment: a critical revision of the currently available tools. *European journal of cancer*. 2010;46(3):479-94.

Cavaletti G, Marmiroli P. Chemotherapy-induced peripheral neurotoxicity. *Nature reviews, neurology*. 2010;6(12):657-66.

Cavaletti G, Cornblath DR, Merkies ISJ, et al. The chemotherapy-induced peripheral neuropathy outcome measures standardization study: from consensus to the first validity and reliability findings. *Annals of Oncology*. 2013;24(2):454-462.

Cavaletti G, Alberti P, Marmiroli P. Chemotherapy-induced peripheral neurotoxicity in cancer survivors: an underdiagnosed clinical entity? *American Society of Clinical Oncology Educational Book*. 2015:e553-60

Cavaletti G, Marmiroli P. Chemotherapy-induced peripheral neurotoxicity. *Current opinion in neurology*. 2015;28(5):500-7.

Cavaletti G, Marmiroli P. Pharmacotherapy options for managing chemotherapy-induced peripheral neurotoxicity. *Expert opinionoin pharmacotherapy*. 2018;19(2):113-121.

Chau I, Cunningham D. Oxaliplatin for colorectal cancer in the United States: better late than never. *Journal of clinical oncology*. 2003;21(11):2049-51.

Cheng YM, Claydon TW. Voltage-dependent gating of HERG potassium channels. *Frontiers in Pharmacology*. 2012;3:83.

Chiorazzi A, Semperboni S, Marmiroli P. Current View in Platinum Drug Mechanisms of Peripheral Neurotoxicity. *Toxics*. 2015;3(3):304-321.

Chiesa N, Rosati B, Arcangeli A, Olivotto M, Wanke E. A novel role for HERG K^+ channels: spike-frequency adaptation. *Journal of physiology*. 1997;501:313–318.

Cersosimo RJ. Oxaliplatin-associated neuropathy: a review. *The annals of pharmacotherapy*.2005;39(1):128-35.

Cerri S, Piccolini VM, Santin G, Bottone MG, De Pascali SA, Migoni D, Iadarola P, Fanizzi FP, Bernocchi G. The developmental neurotoxicity study of platinum compounds. Effects of cisplatin versus a novel Pt(II) complex on rat cerebellum. *Neurotoxicology and teratology*. 2011;33(2):273-81.

Cornblath DR, Chaudhry V, Carter K, et al. Total neuropathy score: validation and reliability study. *Neurology*. 1999;53:1660-1664

Cunningham D, Starling N, Rao S, Iveson T, Nicolson M, Coxon F, Middleton G, Daniel F, Oates J, Norman AR; Upper Gastrointestinal Clinical Studies Group of the National Cancer Research Institute of the United Kingdom. Capecitabine and oxaliplatin for advanced esophagogastric cancer. *The New England journal of medicine*. 2008;358(1):36-46.

Curran ME, Splawski I, Timothy KW, Vincent GM, Green ED, Keating MT. A molecular basis for cardiac arrhythmia: HERG mutations cause long QT syndrome. *Cell*. 1995;80(5):795-803.

Dasari S, Tchounwou PB. Cisplatin in cancer therapy: molecular mechanisms of action. *European journal of pharmacology*. 2014;740:364-78.

Deuis JR, Zimmermann K, Romanovsky AA, Possani LD, Cabot PJ, Lewis RJ, Vetter I. An animal model of oxaliplatin-induced cold allodynia reveals a crucial role for Nav1.6 in peripheral pain pathways. *Pain*. 2013;154(9):1749-57.

de Gramont A, Figer A, Seymour M, Homerin M, Hmissi A, Cassidy J, Boni C, Cortes-Funes H, Cervantes A, Freyer G, Papamichael D, Le Bail N, Louvet C, Hendler D, de Braud F, Wilson C, Morvan F, Bonetti A. Leucovorin and fluorouracil with or without oxaliplatin as first-line

treatment in advanced colorectal cancer. *Journal of clinical oncology*. 2000;18(16):2938-47.

De Monaco A,Valente D, Di Paolo M, Troisi A, D'Orta A, Del Buono A. Oxaliplatin-based therapy: strategies to prevent or minimize neurotoxicity. *World Cancer Research Journal*. 2014;1(2):e232.

Di Francesco AM, Ruggiero A, Riccardi R. Cellular and molecular aspects of drugs of the future: oxaliplatin. *Cellular molecular life science*. 2002;59(11):1914-27.

Eastman A. Glutathione-mediated activation of anticancer platinum(IV) complexes. *Biochemical pharmacology*. 1987;36(23):4177-8.

Ehrsson H, Wallin I, Yachnin J. Pharmacokinetics of oxaliplatin in humans. Medical oncology. 2002;19(4):261-5.

Eijkelkamp N, Linley JE, Baker MD, Minett MS, Cregg R, Werdehausen R, Rugiero F, Wood JN. Neurological perspectives on voltage-gated sodium channels. *Brain*. 2012;135(Pt 9):2585-612.

el-Khateeb M, Appleton TG, Gahan LR, Charles BG, Berners-Price SJ, Bolton AM. Reactions of cisplatin hydrolytes with methionine, cysteine, and plasma ultrafiltrate studied by a combination of HPLC and NMR techniques. *Journal of inorganic biochemistry*. 1999;77(1-2):13-21.

Extra JM, Marty M, Brienza S, Misset JL. Pharmacokinetics and safety profile of oxaliplatin. *Seminars in oncology*. 1998;25(2 Suppl 5):13-22.

Faivre S, Chan D, Salinas R, Woynarowska B, Woynarowski JM. DNA strand breaks and apoptosis induced by oxaliplatin in cancer cells. *Biochemical pharmacology*. 2003;66(2):225-37.

Faravelli L, Arcangeli A, Olivotto M, Wanke E. A HERG-like K+ channel in rat F-11 DRG cell line: pharmacological identification and biophysical characterization. *Journal of physiology*. 1996;496 (Pt 1):13-23.

Filipski KK, Mathijssen RH, Mikkelsen TS, Schinkel AH, Sparreboom A. Contribution of organic cation transporter 2 (OCT2) to cisplatin-induced nephrotoxicity. *Clin Pharmacol Ther*. 2009;86(4):396-402.

Fujita S, Hirota T, Sakiyama R, Baba M, Ieiri I. Identification of drug transporters contributing to oxaliplatin-induced peripheral neuropathy. *Journal of neurochemistry*. 2018.

Fukuda Y, Li Y, Segal RA. A Mechanistic Understanding of Axon Degeneration in Chemotherapy-Induced Peripheral Neuropathy. *Frontiers in Neuroscience*. 2017;11:481.

Gamelin E, Gamelin L, Bossi L, Quasthoff S. Clinical aspects and molecular basis of oxaliplatin neurotoxicity: current management and development of preventive measures. *Seminars in oncology*. 2002;29(5 Suppl 15):21-33.

Geldof AA, Minneboo A, Heimans JJ. Vinca-alkaloid neurotoxicity measured using an in vitro model. *Journal of neurooncology*. 1998;37(2):109-13.

George A, Bostock H. Multiple measures of axonal excitability in peripheral sensory nerves: an in vivo rat model. *Muscle and nerve*. 2007;36(5):628-36.

Gill JS, Windebank AJ. Cisplatin-induced apoptosis in rat dorsal root ganglion neurons is associated with attempted entry into the cell cycle. *Journal of clinical investigation*. 1998;101:2842–2850.

Goodsell D.S. The molecular perspective: Cisplatin. *Stem Cells.* 2006;24(3):514-5.

Graham MA, Lockwood GF, Greenslade D, Brienza S, Bayssas M, Gamelin E. Clinical pharmacokinetics of oxaliplatin: a critical review. *Clinical cancer research*.2000;6(4):1205-18.

Grolleau F, Gamelin L, Boisdron-Celle M, Lapied B, Pelhate M, Gamelin E. A possible explanation for a neurotoxic effect of the anticancer agent oxaliplatin on neuronal voltage-gated sodium channels. *Journal Neurophysiology*. 2001;85(5):2293-7.

Grothey A. Oxaliplatin-safety profile: neurotoxicity. *Seminars in oncology*. 2003;30(4 Suppl 15):5-13.

Guasti L, Cilia E, Crociani O, Hofmann G, Polvani S, Becchetti A, Wanke E, Tempia F, Arcangeli A. Expression pattern of the ether-a-go-go-related (ERG) family proteins in the adult mouse central nervous system: evidence for coassembly of different subunits. *The journal of comparatve neurology*. 2005;491(2):157-74.

Harrap KR. Preclinical studies identifying carboplatin as a viable cisplatin alternative. *Cancer treatment reviews*.1985;12(Suppl A):21–33.

Hartmann JT, Lipp HP. Toxicity of platinum compounds. *Expert opinion on pharmacotherapy*. 2003;4(6):889-901.

Hausheer FH, Schilsky RL, Bain S, Berghorn EJ, Lieberman F. Diagnosis, management, and evaluation of chemotherapy-induced peripheral neuropathy. *Seminary in Oncology.* 2006;33(1):15–49.

Henley SJ, Singh SD, King J, Wilson RJ, O'Neil ME, Ryerson AB. Invasive Cancer Incidence and Survival - United States, 2013. *MMWR Morbidity and mortality weekly report.* 2017;66(3):69-75.

Hershman DL, Weimer LH, Wang A, Kranwinkel G, Brafman L, Fuentes D, Awad D, Crew KD. Association between patient reported outcomes and

quantitative sensory tests for measuring long-term neurotoxicity in breast cancer survivors treated with adjuvant paclitaxel chemotherapy. *Breast cancer research and treatment*. 2011;125(3):767-74.

Hershman DL, Lacchetti C, Dworkin RH, Lavoie Smith EM, Bleeker J, Cavaletti G, Chauhan C, Gavin P, Lavino A, Lustberg MB, Paice J, Schneider B, Smith ML, Smith T, Terstriep S, Wagner-Johnston N, Bak K, Loprinzi CL; American Society of Clinical Oncology. Prevention and management of chemotherapy-induced peripheral neuropathy in survivors of adult cancers: American Society of Clinical Oncology clinical practice guideline. *Journal of clinical oncology*. 2014;32(18):1941-67.

Hershman DL, Till C, Wright JD, Awad D, Ramsey SD, Barlow WE, Minasian LM, Unger J. Comorbidities and risk of chemotherapy-induced peripheral neuropathy among participants 65 years or older in southwest oncology group clinical trials. *Journal of clinical oncology*. 2016;34(25):3014-22.

Higby DJ, Wallace HJ Jr, Albert DJ, Holland JF. Diaminodichloroplatinum: a phase I study showing responses in testicular and other tumors. *Cancer*. 1974;33(5):1219-5.

Hoeijmakers JG, Faber CG, Lauria G, Merkies IS, Waxman SG. Small fibre neuropathies–advances in diagnosis, pathophysiology and management. *Nature reviews neurology*. 2012;8:369-379.

Hopkins HL, Duggett NA, Flatters SJL. Chemotherapy-induced painful neuropathy: pain-like behaviours in rodent models and their response to commonly used analgesics. *Current opinion in supportive and palliative care*. 2016 Jun;10(2):119-128.

Howell SB, Safaei R, Larson CA, Sailor MJ. Copper transporters and the cellular pharmacology of the platinum-containing cancer drugs. *Molecular pharmacology*. 2010;77(6):887-94.

Imai S, Koyanagi M, Azimi Z, Nakazato Y, Matsumoto M, Ogihara T, Yonezawa A, Omura T, Nakagawa S, Wakatsuki S, Araki T, Kaneko S, Nakagawa T, Matsubara K. Taxanes and platinum derivatives impair Schwann cells via distinct mechanisms. *Scientific Reports*. 2017;7(1):5947.

Jaggi AS, Singh N. Mechanisms in cancer-chemotherapeutic drugs-induced peripheral neuropathy. *Toxicology*. *2012;291(1-3):1-9.*

Jamieson ER, Lippard SJ. Structure, recognition, and processing of cisplatin-DNA Adducts. *Chemical reviews*. 1999; 99(9):2467-98.

Jimenez-Andrade JM, Herrera MB, Ghilardi JR, Vardanyan M, Melemedjian OK, Mantyh PW. Vascularization of the dorsal root ganglia and peripheral nerve of the mouse: implications for chemical-induced peripheral sensory neuropathies. *Molecular pain*. 2008;4:10.

Johnstone TC, Suntharalingam K, Lippard SJ. The next generation of platinum drugs: targeted Pt(II) agents, nanoparticle delivery, and Pt(IV) prodrugs. *Chemical reviews*. 2016;116(5):3436-86.

Kagiava A, Tsingotjidou A, Emmanouilides C, Theophilidis G. The effects of oxaliplatin, an anticancer drug, on potassium channels of the peripheral myelinated nerve fibres of the adult rat. *Neurotoxicology*. 2008;29(6):1100-6.

Kagiava A, Kosmidis EK, Theophilidis G. Oxaliplatin-induced hyperexcitation of rat sciatic nerve fibers: an intra-axonal study. *Anticancer agents in medical chemistry*. 2013;13(2):373-9.

Kagiava A, Theophilidis G, Sargiannidou I, Kyriacou K, Kleopa KA. Oxaliplatin-induced neurotoxicity is mediated through gap junction channels and hemichannels and can be prevented by octanol. *Neuropharmacology*. 2015t;97:289-305.

Kelland LR. New platinum antitumor complexes. Critical reviews in oncology/hematology. 1993;15(3):191-219.

Kelland LR. A new resistance mechanism to cisplatin? *Drug resistance updates*. 2000;3(3):139-141.

Kelland L. The resurgence of platinum-based cancer chemotherapy. Nature *reviews. Cancer*. 2007;7(8):573-84.

Kerckhove N, Collin A, Condé S, Chaleteix C, Pezet D, Balayssac D. Long-term effects, pathophysiological mechanisms, and risk factors of chemotherapy-induced peripheral neuropathies: a comprehensive literature review. *Frontiers in Pharmacology*. 2017;8:86.

Kim PY, Johnson CE. Chemotherapy-induced peripheral neuropathy: a review of recent findings. *Current opinion in anaesthesiology*. 2017;30(5):570-576.

Komatsu M, Sumizawa T, Mutoh M, Chen ZS, Terada K, Furukawa T, Yang XL, Gao H, Miura N, Sugiyama T, Akiyama S. Copper-transporting P-type adenosine triphosphatase (ATP7B) is associated with cisplatin resistance. *Cancer research.* 2000;60(5):1312-6.

Krishnan AV, Goldstein D, Friedlander M, Kiernan MC. Oxaliplatin induced neurotoxicity and the development of neuropathy. *Muscle and nerve*. 2005; 32:51–60.

Krishnan AV, Goldstein D, Friedlander M, Kiernan MC. Oxaliplatin and axonal Na^+ channel function in vivo. *Clinical cancer research.* 2006; 12:4481–4.

Knox RJ, Friedlos F, Lydall DA, Roberts JJ. Mechanism of cytotoxicity of anticancer platinum drugs: evidence that cis-diamminedichloroplatinum(II) and cis-diammine-(1,1-cyclobutanedicarboxylato)platinum(II) differ only in

the kinetics of their interaction with DNA. *Cancer Research*. 1986; 46(4 Pt 2):1972-9.

Lehky TJ, Leonard GD, Wilson RH, Grem JL, Floeter MK. Oxaliplatin-induced neurotoxicity: acute hyperexcitability and chronic neuropathy. *Muscle and Nerve*. 2004;29:387-92.

Leo M, Schmitt LI, Erkel M, Melnikova M, Thomale J, Hagenacker T. Cisplatin-induced neuropathic pain is mediated by upregulation of N-type voltage-gated calcium channels in dorsal root ganglion neurons. *Experimental neurology*. 2017;288:62-74.

Lin X, Okuda T, Holzer A, Howell SB. The copper transporter CTR1 regulates cisplatin uptake in Saccharomyces cerevisiae. *Molecular pharmacology*. 2002;62(5):1154-9.

Liu JJ, Jamieson SM, Subramaniam J, Ip V, Jong NN, Mercer JF, McKeage MJ. Neuronal expression of copper transporter 1 in rat dorsal root ganglia: association with platinum neurotoxicity. *Cancer chemotherapy pharmacology*. 2009;64(4):847-56.

Lolignier S, Bonnet C, Gaudioso C, Noël J, Ruel J, Amsalem M, Ferrier J, Rodat-Despoix L, Bouvier V, Aissouni Y, Prival L, Chapuy E, Padilla F, Eschalier A, Delmas P, Busserolles J. The Nav1.9 channel is a key determinant of cold pain sensation and cold allodynia. *Cell repor*ts. 2015;11(7):1067-78.

Louvet C, Labianca R, Hammel P, Lledo G, Zampino MG, André T, Zaniboni A, Ducreux M, Aitini E, Taïeb J, Faroux R, Lepere C, de Gramont A; GERCOR; GISCAD. Gemcitabine in combination with oxaliplatin compared with gemcitabine alone in locally advanced or metastatic pancreatic cancer: results of a GERCOR and GISCAD phase III trial. *Journal of clinical oncology*. 2005;23(15):3509-16.

Luo FR, Wyrick SD, Chaney SG. Comparative neurotoxicity of oxaliplatin, ormaplatin, and their biotransformation products utilizing a rat dorsal root ganglia in vitro explant culture model. *Cancer chemotheraphy and pharmacology*. 1999;44(1):29-38.

Malgrange B, Delree P, Rigo J, Baron H, Moonen G. Image analysis of neuritic regeneration by adult rat dorsal root ganglion neurons in culture: quantification of the neurotoxicity of anticancer agents and of its prevention by nerve growth factor or basic fibroblast growth factor but not brain-derived neurotrophic factor or neurotrophin-3. *Journal of neuroscience methods*. 1994;53:111–122.

Marmiroli P, Nicolini G, Miloso M, Scuteri A, Cavaletti G. The fundamental role of morphology in experimental neurotoxicology: the example of chemotherapy-induced peripheral neurotoxicity. *Italian journal of anatomy and embryology*. 2012;117(2):75-97.

Marmiroli P, Scuteri A, Cornblath DR, Cavaletti G. Pain in chemotherapy-induced peripheral neurotoxicity. *Journal of peripheral nervous system*. 2017;22(3):156-161.

Mathé G, Kidani Y, Segiguchi M, Eriguchi M, Fredj G, Peytavin G, Misset JL, Brienza S, de Vassals F, Chenu E, et al. Oxalato-platinum or 1-OHP, a third-generation platinum complex: an experimental and clinical appraisal and preliminary comparison with cis-platinum and carboplatinum. *Biomedicine and pharmacotheraphy*. 1989;43(4):237-50.

McWhinney SR, Goldberg RM, McLeod HL. Platinum neurotoxicity pharmacogenetics. *Molecular cancer therapeutics*. 2009;8(1):10-6.

Meregalli C, Fumagalli G, Alberti P, Canta A, Carozzi VA, Chiorazzi A, Monza L, Pozzi E, Sandelius Å, Blennow K, Zetterberg H, Marmiroli P, Cavaletti G. Neurofilament light chain as disease biomarker in a rodent model of chemotherapy induced peripheral neuropathy. *Experimental neurology*. 2018;307:129-132.

Miltenburg NC, Boogerd W. Chemotherapy-induced neuropathy: A comprehensive survey. *Cancer treatment reviews*. 2014;40(7):872-82.

Monneret C. Platinum anticancer drugs. From serendipity to rational design. *Annales pharmaceutiques francaises*. 2011;69(6):286-95.

Mustafa Ali M, Moeller M, Rybicki L, Moore HCF. Long-term peripheral neuropathy symptoms in breast cancer survivors. *Breast cancer research and treatment*. 2017;166(2):519-526.

Nakagawa-Yagi Y, Choi DK, Ogane N, Shimada S, Seya M, Momoi T, Ito T, Sakaki Y. Discovery of a novel compound: insight into mechanisms for acrylamide-induced axonopathy and colchicine-induced apoptotic neuronal cell death. *Brain research*. 2001;909(1-2):8-19.

Nishida K, Takeuchi K, Hosoda A, Sugano S, Morisaki E, Ohishi A, Nagasawa K. Ergothioneine ameliorates oxaliplatin-induced peripheral neuropathy in rats. *Life Sciences*. 2018;207:516-524.

Nodera H, Spieker A, Sung M, Rutkove S. Neuroprotective effects of Kv7 channel agonist, retigabine, for cisplatin-induced peripheral neuropathy. *Neuroscience letters*. 2011;505(3):223-7.

Oun R, Moussa YE, Wheate NJ. The side effects of platinum-based chemotherapy drugs: a review for chemists. *Dalton transactions*. 2018;47(19):6645-6653.

Park SB, Krishnan AV, Lin C, Goldstein D, Friedlander M, Kiernan MC. Mechanisms underlying chemotherapy-induced neurotoxicity and the potential for neuroprotective strategies. *Current medicinal chemistry*. 2008;15(29): 3081-3094.

Park SB, Goldstein D, Lin CS, Krishnan AV, Friedlander ML, Kiernan MC. Acute abnormalities of sensory nerve function associated with oxaliplatin-induced neurotoxicity. *Journal of clinical oncology*. 2009;27(8):1243-9.

Park SB, Goldstein D, Krishnan AV, Lin CS, Friedlander ML, Cassidy J, Koltzenburg M, Kiernan MC. Chemotherapy-induced peripheral neurotoxicity: a critical analysis. *CA: A cancer journal for clinicians.* 2013;63(6):419-37.

Pietrangeli A, Leandri M, Terzoli E, Jandolo B, Garufi C. Persistence of high-dose oxaliplatin-induced neuropathy at long-term follow-up. *European neurology*. 2006;56(1):13-6.

Pike CT, Birnbaum HG, Muehlenbein CE, Pohl GM, Natale RB. Healthcare costs and workloss burden of patients with chemotherapy-associated peripheral neuropathy in breast, ovarian, head and neck, and nonsmall cell lung cancer. *Chemotherapy Research and Practice*.2012:913848.

Pillozzi S, D'Amico M, Bartoli G, Gasparoli L, Petroni G, Crociani O, Marzo T, Guerriero A, Messori L, Severi M, Udisti R, Wulff H, Chandy KG, Becchetti A, Arcangeli A. The combined activation of K(Ca)3.1 and inhibition of K(v)11.1/hERG1 currents contribute to overcome Cisplatin resistance in colorectal cancer cells. *British journal of cancer*. 2018 Jan;118(2):200-212.

Pinto AL, Lippard SJ. Binding of the antitumor drug cis-diamminedichloroplatinum(II) (cisplatin) to DNA. *Biochimica et biophysica acta*.1985;780(3):167-80.

Pittman SK, Gracias NG, Vasko MR, Fehrenbacher JC. Paclitaxel alters the evoked release of calcitonin gene-related peptide from rat sensory neurons in culture. *Experimental neurology*. 2013;253C: 146–153.

Platika D, Boulos MH, Baizer L, Fishman MC. Neuronal traits of clonal cell lines derived by fusion of dorsal root ganglia neurons with neuroblastoma cells. *Proceedings of the National Academy of Sciences*. 1985;82(10):3499-3503.

Poupon L, Lamoine S, Pereira V, Barriere DA, Lolignier S, Giraudet F, Aissouni Y, Meleine M, Prival L, Richard D, Kerckhove N, Authier N, Balayssac D, Eschalier A, Lazdunski M, Busserolles J. Targeting the TREK-1 potassium channel via riluzole to eliminate the neuropathic and depressive-like effects of oxaliplatin. *Neuropharmacology*. 2018;140:43-61.

Puckett CA, Ernst RJ, Barton JK. Exploring the cellular accumulation of metal complexes. *Dalton Transactions*. 2010;39(5):1159-70.

Pulvers JN, Marx G. Factors associated with the development and severity of oxaliplatin-induced peripheral neuropathy: a systematic review. *Asia-pacific journal of clinical oncology*. 2017;13(6):345-355.

Raymond E, Faivre S, Woynarowski JM, Chaney SG. Oxaliplatin: mechanism of action and antineoplastic activity. *Seminars in oncology*. 1998;25(2 Suppl 5):4-12.

Rogers M, Tang L, Madge DJ, Stevens EB. The role of sodium channels in neuropathic pain. *Seminars in cell and developmental biology*. 2006;17(5):571-81.

Rosati B, Marchetti P, Crociani O, Lecchi M, Lupi R, Arcangeli A, Olivotto M, Wanke E. Glucose- and arginine-induced insulin secretion by human pancreatic beta-cells: the role of HERG K(+) channels in firing and release. *FASEB Journal*. 2000;14(15):2601-10.

Rosenberg B, Vancamp L, Krigas T. Inhibition of cell division in Escherichia Coli by electrolysis products from a platinum electrode. *Nature*. 1965;205:698-9.

Rosenberg B, VanCamp L, Trosko JE, Mansour VH. Platinum compounds: a new class of potent antitumour agents. *Nature*. 1969;222(5191):385-6.

Samimi G, Katano K, Holzer AK, Safaei R, Howell SB. Modulation of the cellular pharmacology of cisplatin and its analogs by the copper exporters ATP7A and ATP7B. *Molecular pharmacology*. 2004;66(1):25-32.

Saganich MJ, Machado E, Rudy B. Differential expression of genes encoding subthreshold-operating voltage-gated K+ channels in brain. *The journal of neuroscience*. 2001;21(13):4609-24.

Schmitt LI, Leo M, Kleinschnitz C, Hagenacker T. Oxaliplatin Modulates the Characteristics of Voltage-Gated Calcium Channels and Action Potentials in Small Dorsal Root Ganglion Neurons of Rats. *Molecular neurobiology*. 2018.

Screnci D, McKeage MJ, Galettis P, Hambley TW, Palmer BD, Baguley BC. Relationships between hydrophobicity, reactivity, accumulation and peripheral nerve toxicity of a series of platinum drugs. *British journal of cancer*. 2000;82(4):966-72.

Scuteri A, Galimberti A, Maggioni D, Ravasi M, Pasini S, Nicolini G, Bossi M, Miloso M, Cavaletti G, Tredici G. Role of MAPKs in platinum-induced neuronal apoptosis. *Neurotoxicology*.2009;30(2),312-319.

Sereno M, Gutiérrez-Gutiérrez G, Rubio JM, Apellániz-Ruiz M, Sánchez-Barroso L, Casado E, Falagan S, López-Gómez M, Merino M, Gómez-Raposo C, Rodriguez-Salas N, Tébar FZ, Rodríguez-Antona C. Genetic polymorphisms of SCN9A are associated with oxaliplatin-induced neuropathy. *BMC Cancer*. 2017;17(1):63.

Seretny M, Currie GL, Sena ES, Ramnarine S, Grant R, MacLeod MR, Colvin LA, Fallon M. Incidence, prevalence, and predictors of chemotherapy-induced peripheral neuropathy: A systematic review and

meta-analysis. *Pain*. 2014;155(12):2461-70.

Sharma M, Sharma P, Pant HC. CDK-5-mediated neurofilament phosphorylation in SHSY5Y human neuroblastoma cells. *Journal of neurochemistry*. 1999;73(1):79-86.

Shi W, Wymore RS, Wang HS, Pan Z, Cohen IS, McKinnon D, Dixon JE. Identification of two nervous system-specific members of the erg potassium channel gene family. *The journal of neuroscience*. 1997;17(24):9423-32.

Siddik ZH. Cisplatin: mode of cytotoxic action and molecular basis of resistance. *Oncogene*. 2003;22(47):7265-79.

Siegel RL, Miller KD, Jemal A. Cancer statistics, 2018. *CA: A cancer journal for clinicians*. 2018;68(1):7-30.

Sittl R, Lampert A, Huth T, Schuy ET, Link AS, Fleckenstein J, Alzheimer C, Grafe P, Carr RW. Anticancer drug oxaliplatin induces acute cooling-aggravated neuropathy via sodium channel subtype Na(V)1.6-resurgent and persistent current. *Proceedings of the national academy of science of the United States of America*. 2012;109(17):6704-9.

Sittl R, Carr RW, Fleckenstein J, Grafe P. Enhancement of axonal potassium conductance reduces nerve hyperexcitability in an in vitro model of oxaliplatin-induced acute neuropathy. *Neurotoxicology*. 2010;31(6):694-700.

Snyder C, Yu L, Ngo T, Sheinson D, Zhu Y, Tseng M, Misner D, Staflin K. In vitro assessment of chemotherapy-induced neuronal toxicity. *Toxicology in vitro*. 2018 Aug;50:109-123.

Sprowl JA, Ciarimboli G, Lancaster CS, et al. Oxaliplatin-induced neurotoxicity is dependent on the organic cation transporter OCT2. *Proceedings of the national academy of science of the United States of America*. 2013;110(27):11199-204.

Staff NP, Grisold A, Grisold W, Windebank AJ. Chemotherapy-induced peripheral neuropathy: A current review. *Annals of neurology*. 2017;81(6):772-781.

Starobova H, Vetter I. Pathophysiology of Chemotherapy-Induced Peripheral Neuropathy. *Frontiers in molecular neuroscience*. 2017;10:174.

Themistocleous AC, Ramirez JD, Serra J, Bennett DL. The clinical approach to small fibre neuropathy and painful channelopathy. *Practical Neurology*. 2014;14:368–379.

Todd RC, Lippard SJ. Inhibition of transcription by platinum antitumor compounds. *Metallomics*. 2009;1(4):280-91.

Tomaszewski A, Büsselberg D. Cisplatin modulates voltage gated channel currents of dorsal root ganglion neurons of rats. *Neurotoxicology*. 2007;28(1):49-58. Epub 2006 Jul 20.

Velasco R, Bruna J, Briani C, Argyriou AA, Cavaletti G, Alberti P, Frigeni B, Cacciavillani M, Lonardi S, Cortinovis D, Cazzaniga M, Santos C, Kalofonos HP. Early predictors of oxaliplatin-induced cumulative neuropathy in colorectal cancer patients. *Journal of Neurology, neurosurgery and psychiatry*. 2014;85(4):392–8.

Verberne CJ, Wiggers T, Vermeulen KM., de Jong KP. Detection of recurrences during follow-up after liver surgery for colorectal metastases: Both carcinoembryonic antigen (CEA) and imaging are important. *Annals of surgical oncology*. 2013;20:457-463.

Verstappen CC, Postma TJ, Geldof AA, Heimans JJ. Amifostine protects against chemotherapy-induced neurotoxicity: an in vitro investigation. *Anticancer research*. 2004;24(4):2337-41.

Viatchenko-Karpinski V, Ling J, Gu JG. Down-regulation of Kv4.3 channels and a-type K(+) currents in V2 trigeminal ganglion neurons of rats following oxaliplatin treatment. *Molecular pain*. 2018;14:1744806917750995.

Villa D, Miloso M, Nicolini G, Rigolio R, Villa A, Cavaletti G, Tredici G. Low-dose cisplatin protects human neuroblastoma SH-SY5Y cells from paclitaxel-induced apoptosis. *Molecular cancer therapeuthics*. 2005;4:1439-1447.

Wainger BJ, Buttermore ED, Oliveira JT, Mellin C, Lee S, Saber WA, Wang AJ, Ichida JK, Chiu IM, Barrett L, Huebner EA, Bilgin C, Tsujimoto N, Brenneis C, Kapur K, Rubin LL, Eggan K, Woolf CJ. Modeling pain in vitro using nociceptor neurons reprogrammed from fibroblasts. *Nature neuroscience*. 2015; 18(1):17–24.

Warmke JW, Ganetzky B. A family of potassium channel genes related to eag in Drosophila and mammals. Proceedings of the natural academy of science of the U S A. 1994;91(8):3438-42.

Webster R.G., Brain K.L., Wilson R.H., Grem J.L., Vincent A. Oxaliplatin induces hyperexcitability at motor and autonomic neuromuscular junctions through effects on voltage-gated sodium channels. *British Journal of Pharmacology*. 2005;146(7):1027-39.

Weiss RB, Christian MC. New cisplatin analogues in development. A review. *Drugs*. 1993;46(3):360-377.

Wessig C, Bendszus M, Reiners K, Pham M. Lesions of the peripheral nerves: MR neurography as an innovative supplement to electrodiagnostics. *Klinische Neurophysiologie.* 2011;42:231-238.

Wheeler HE, Wing C, Delaney SM, Komatsu M, Dolan ME. Modeling chemotherapeutic neurotoxicity with human induced pluripotent stem cell-derived neuronal cells. *PLoS One.* 2015;10(2):e0118020.

Wilson RH, Lehky T, Thomas RR, Quinn MG, Floeter MK, Grem JL. Acute

oxaliplatin-induced peripheral nerve hyperexcitability. *Journal of clinical oncology*. 2002;20(7):1767-74.

Wolf S, Barton D, Kottschade L, Grothey A, Loprinzi C. Chemotherapy-induced peripheral neuropathy: prevention and treatment strategies. *European journal of cancer*. 2008;44(11):1507-15.

Wu SN, Chen BS, Wu YH, Peng H, Chen LT. The mechanism of the actions of oxaliplatin on ion currents and action potentials in differentiated NG108-15 neuronal cells. *Neurotoxicology*. 2009;30(4):677-85.

Zhang S, Lovejoy KS, Shima JE, et al. Organic cation transporters are determinants of oxaliplatin cytotoxicity. *Cancer research*. 2006;66(17):8847-57.

Zwelling LA, Anderson T, Kohn KW. DNA-protein and DNA interstrand cross-linking by cis- and trans-platinum(II) diamminedichloride in L1210 mouse leukemia cells and relation to cytotoxicity. *Cancer Research*. 1979; 39(2 Pt 1):365-9.